ASSESSING THE EFFECTS OF GENETIC MODIFICATIONS ON PHOTOSYNTHETIC CAPACITY IN *NICOTIANA TABACUM* (TOBACCO) AND *GLYCINE MAX* (SOYBEAN)

BY

NOEL LENNON PIATEK

THESIS

Submitted in partial fulfillment of the requirements
for the degree of Master of Science in Plant Biology
in the Graduate College of the
University of Illinois at Urbana-Champaign, 2015

Urbana, Illinois

Adviser:

Professor Stephen Long

ABSTRACT

The global population is projected to exceed nine billion people by the year 2050, which means an ever-increasing strain on the world's natural resources, especially food, fuel, and fiber. The challenge comes with trying to produce more food crops on the same amount of land while maintaining or lessening the amount of inputs, including water and fertilizer. One avenue for meeting this demand is to engineer increased photosynthetic conversion efficiency to in turn increase genetic yield potential, which is defined as the maximum amount of yield a plant can produce in optimal growing conditions based on genetics.

This study assesses the resulting plants from two different approaches to increase photosynthetic conversion efficiency. The first approach explores five transformations of *Nicotiana tabacum* cv. Petite Havana. Three of the transformations encode different changes in the binding specificity of ribulose-1,5-bisphosphate carboxylase/oxygenase for carbon dioxide, one encodes a gene for expression of a bicarbonate transporter, and one overexpresses the native rubisco by 15%. Plants were phenotyped in an agricultural field trial and then in two controlled environment experiments. It was predicted that these modifications would increase rubisco-limited photosynthesis. No comparisons made between wild type tobacco and the modified tobacco types were shown to be significantly better in the modified tobacco types. For this reason, determining the rubisco activation rates of the lines that have an altered binding specificity for CO_2 at a range of temperatures would inform how these changes are altering rubisco kinetics on a molecular scale and could inform future decisions about modifications to rubisco.

The second approach explores two transformations of *Glycine max* cv. Thorne. One transformation encodes a cyanobacterial gene that affects carbon dioxide concentrations around

rubisco and the other encodes a cyanobacterial gene fructose-1,6-bisphosphate/sedoheptulose-bisphosphatase. Plants were examined in two controlled environment experiments in addition to an agricultural field trial. This approach has multiple predictions. 1) Expressing the *ictB* gene increases rates of rubisco-limited photosynthesis and RuBP regeneration-limited photosynthesis. 2) Expressing the *SBFB* gene will show significantly increased RuBP regeneration-limited photosynthesis. No comparisons made between wild type soybean and the modified soybean types were shown to be significantly better in the modified soybeans. In the cases of *ictB* and *SBFB* genes, it would be beneficial to elucidate their functions in cyanobacteria before transforming them into higher plants again. Fully understanding their function and mechanism would allow for the optimization of introducing such cyanobacterial genes into higher plants. Though the genetic alterations made to the plants in this study did not have the predicted outcomes based on previous research, this study has potentially contributed to the knowledge of which genes do and do not have strong impacts on photosynthetic capacity and efficiency.

“Life’s a garden, dig it” – Joe Dirt

ACKNOWLEDGEMENTS

I would like to give a special thanks to my adviser, Steve, who has been endlessly patient, kind, and supportive during my time at the University of Illinois. I would also like to thank Dr. Lisa Ainsworth and Dr. Don Ort for agreeing to be on my committee. I'd like to thank all the members of the Long lab for their help and good nature over the past two years. I'd especially like to thank Rachel for putting up with my crazy, Wanne and Kasia for finding time in between making fun of me to teach me a lab technique or two, and Idan, Lynn, and Charles for being great sources of advice and laughter. I'm thankful to David Drag for assistance in the field trials. I'm also grateful to Tom Clemente for providing the transgenic soybean seeds and Spencer Whitney for providing the transgenic tobacco seeds. Finally, I'm thankful for the Gutsgell Endowment, which provided the financial support for my research assistantship.

TABLE OF CONTENTS

CHAPTER 1: GENERAL INTRODUCTION

Introduction

With the global population expected to reach 9.5 billion by the year 2050, combined with changing diets, the supply of primary foodstuffs needs to double (USCB, 2015). Maize, rice, wheat, and soybean account for ~66% of global calories, but are not increasing at the required 2.4% per year rate needed to double production by 2050 (Ray et al., 2013). Additionally, global production of maize, rice, and wheat may be stagnating (Ray et al., 2013), with 24-39% of the areas that grow these crops showing yields that have either stagnated or declined (Ray et al., 2012). Other factors that will affect crop yields, such as drought, extreme weather events, and ozone are all slated to increase in the future (IPPC, 2014). The anthropogenic emissions of carbon dioxide (CO_2) that were once thought to improve crop yields, have been shown to result in negligible improvements in yield for C_4 crops while effects on C_3 crops were less than anticipated (Long et al., 2006a; Ainsworth et al., 2008). Thus, there are a multitude of challenging issues in the 21st century for achieving food security.

In the past, increases in crop yields have come from expansion of cropland area, increased double cropping, and increasing crop yields per hectare (Foley et al., 2011). Increasing crop yields per hectare was largely achieved through traditional breeding methods such as hybridization, increased planting density, and fertilization schemes. The following equation described here was originally published by Monteith (1977) to describe genetic yield potential (Yp) under optimal management practices and absence of abiotic and biotic stresses: $Yp = 0.487 * S_t * \varepsilon i * \varepsilon c * \varepsilon p$. (Zhu et al., 2010), where S_t is the total incident solar radiation across the growing season, light interception efficiency (εi) of photosynthetically active radiation, conversion efficiency (εc) is the ratio of biomass energy produced over a given period to the

radiative energy intercepted by the canopy over the same period, and partitioning efficiency (εp), which is the amount of total biomass energy partitioned into the harvested portion of the crop. The green revolution of the 1960s largely capitalized on the εi and εp portion of this equation to improve Y_p, providing large yield increases for the major C_3 crops: rice, wheat, and soybean (Long et al., 2006b; Zhu et al., 2010). However, as εi and εp approach their assumed maxima and in light of the various issues for attaining food security in 2050, photosynthetic conversion efficiency will play a larger role in increasing agricultural crop production.

Conversion efficiency depends on the process of net photosynthesis (photosynthesis after respiration is accounted for), which is currently a prime target for improvement after 50 years of intensive basic research into the photosynthetic machinery and process, the advent of high-performance computing, and advanced genetic engineering (Long et al., 2015). Some avenues for enhancing conversion efficiency in C_3 crops include engineering carbon concentrating mechanisms such as those seen in C_4 plants and cyanobacteria, engineering a photorespiratory bypass, relaxing photoinhibition, optimizing canopy structure, optimizing carbon metabolism, and transplanting different rubiscos (ribulose-1,5-bisphosphate carboxylase/oxygenases) (Long et al., 2015). Additional targets include reengineering the photosystems and their collection antennae (Blankenship et al., 2011).

Rubiscos with different binding specificities for CO_2 along with cyanobacterial genes encoding inorganic carbon transporter B (*ictB*) and the bifunctional enzyme fructose-1,6-bisphosphate/sedoheptulose-bisphosphatase (*SBFB*), discussed in the following chapters, have been predicted as targets for improving leaf photosynthesis and conversion efficiency (Long et al., 2006a; Long et al., 2015; Zhu et al., 2010).

Research objectives

Chapter two explores five transformations of *Nicotiana tabacum* cv. Petite Havana. Three of the transformations encode different changes in the binding specificity of rubisco for carbon dioxide, one encodes a gene for expression of a cyanobacterial bicarbonate transporter, and one overexpresses native rubisco by 15%. Plants were phenotyped in an agricultural field trial and then in two controlled environment experiments. It was predicted that these modifications would increase rubisco-limited photosynthesis ($V_{c,max}$), RuBP-limited photosynthesis, net photosynthetic rate (*A*), and productivity relative to the control.

Chapter three explores two transformations of *Glycine max* cv. Thorne. One transformation encodes a cyanobacterial gene that may affect carbon dioxide concentrations around rubisco, *ictB*, and the other encodes the cyanobacterial gene fructose-1,6-bisphosphate/sedoheptulose-bisphosphatase, *SBFB*. Plants were examined in two controlled environment experiments in addition to an agricultural field trial. Chapter three has two predictions. 1) Expressing the *ictB* gene increases rates of rubisco-limited photosynthesis and RuBP regeneration-limited photosynthesis. 2) Expressing the *SBFB* gene will show significant increased RuBP regeneration-limited photosynthesis.

References

Ainsworth, E. A., Leakey, A. D. B., Ort, D. R., & Long, S. P. (2008). FACE-ing the facts: inconsistencies and interdependence among field, chamber and modeling studies of elevated [CO_2] impacts on crop yield and food supply. *New Phytologist, 179*(1), 5-9. doi: 10.1111/j.1469-8137.2008.02500.x

Blankenship, R. E., Tiede, D. M., Barber, J., Brudvig, G. W., Fleming, G., Ghirardi, M., . . . Sayre, R. T. (2011). Comparing Photosynthetic and Photovoltaic Efficiencies and Recognizing the Potential for Improvement. *Science, 332*(6031), 805-809. doi: 10.1126/science.1200165

Foley, J. A., Ramankutty, N., Brauman, K. A., Cassidy, E. S., Gerber, J. S., Johnston, M., . . . Zaks, D. P. M. (2011). Solutions for a cultivated planet. *Nature, 478*(7369), 337-342. doi: 10.1038/nature10452

IPCC. (2014). Climate Change 2014: The Physical Science Basis Contribution of Working Group I to the Fifth Assessment Report of the IPCC. Cambridge University Press, Cambridge UK.

Lieman-Hurwitz, J., Rachmilevitch, S., Mittler, R., Marcus, Y., & Kaplan, A. (2003). Enhanced photosynthesis and growth of transgenic plants that express ictB, a gene involved in HCO_3^- accumulation in cyanobacteria. *Plant Biotechnology Journal, 1*(1), 43-50. doi: 10.1046/j.1467-7652.2003.00003.x

Long, S. P., Ainsworth, E. A., Leakey, A. D. B., Nosberger, J., & Ort, D. R. (2006a). Food for thought: Lower-than-expected crop yield stimulation with rising CO_2 concentrations. *Science, 312*(5782), 1918-1921. doi: 10.1126/science.1114722

Long, S. P., Zhu, X. G., Naidu, S. L., & Ort, D. R. (2006b). Can improvement in photosynthesis increase crop yields? *Plant Cell and Environment, 29*(3), 315-330. doi: 10.1111/j.1365-3040.2005.01493.x

Long, S. P., Marshall-Colon, A., & Zhu, X.-G. (2015). Meeting the global food demand of the future by engineering crop photosynthesis and yield potential. *Cell, 161*(1), 56-66. doi: 10.1016/j.cell.2015.03.019

Miyagawa, Y., Tamoi, M., & Shigeoka, S. (2001). Overexpression of a cyanobacterial fructose-1,6-/sedoheptulose-1,7-bisphosphatase in tobacco enhances photosynthesis and growth. *Nature Biotechnology, 19*(10), 965-969. doi: 10.1038/nbt1001-965

Monteith, J. L. (1977). Climate and the efficiency of crop production in Britain. *Philosophical Transactions of the Royal Society of London Series B-Biological Sciences, 281*(980), 277-294. doi: 10.1098/rstb.1977.0140

USCB. (2015). World Population 1950-2050. International Database (Washington, DC: U.S. Department of Commerce, Census Bureau).

http://www.census.gov/population/international/data/idb/worldpopgraph.php. Accessed 1 May 2015.

Ray, D. K., Mueller, N. D., West, P. C., & Foley, J. A. (2013). Yield trends are insufficient to double global crop production by 2050. *Plos One, 8*(6). doi: 10.1371/journal.pone.0066428

Ray, D. K., Ramankutty, N., Mueller, N. D., West, P. C., & Foley, J. A. (2012). Recent patterns of crop yield growth and stagnation. *Nature Communications, 3*. doi: 10.1038/ncomms2296

Tcherkez, G. G. B., Farquhar, G. D., & Andrews, T. J. (2006). Despite slow catalysis and confused substrate specificity, all ribulose bisphosphate carboxylases may be nearly perfectly optimized. *Proceedings of the National Academy of Sciences of the United States of America, 103*(19), 7246-7251. doi: 10.1073/pnas.0600605103

Tcherkez, G. (2013). Modelling the reaction mechanism of ribulose-1,5-bisphosphate carboxylase/oxygenase and consequences for kinetic parameters. *Plant Cell and Environment, 36*(9), 1586-1596. doi: 10.1111/pce.12066

United Nations. (2014). United Nations Economic and Social Affairs: Concise report on the world population situation in 2014. http://www.un.org/en/development/desa/population/publications/pdf/trends/Concise%20Report%20on%20the%20World%20Population%20Situation%202014/en.pdf. Accessed 1 May 2015.

Zhu, X.-G., Long, S. P., & Ort, D. R. (2010). Improving photosynthetic efficiency for greater yield. *Annual Review of Plant Biology, Vol 61, 61*, 235-261. doi: 10.1146/annurev-arplant-042809-112206

CHAPTER 2: ASSESSING THE EFFECTS OF MODIFIED RUBISCOS INTRODUCED INTO *NICOTIANA TABACUM* CV. PETITE HAVANA

Abstract

Every human on earth is indirectly or directly reliant on photosynthesis to generate food. Ribulose-1,5-bisphosphate carboxylase/oxygenase is responsible for initiating aerobic photosynthetic carbon dioxide assimilation and is the most abundant protein in the world. This study was done to determine how altering the binding specificity of rubisco for carboxylation affects physiological photosynthetic parameters and productivity in *Nicotiana tabacum* cv. Petite Havana. *Nicotiana tabacum* cv. Petite Havana wild type plants along with the transformed lines were grown in an agricultural field setting and controlled environment conditions. Leaf photosynthetic carbon dioxide uptake rates and responses to changes in intercellular carbon dioxide were determined and analyzed. Fresh leaf weights and area were also measured and analyzed. It was found that, in controlled environment conditions, two genotypes showed significantly less Rubisco-limited photosynthetic levels compared to wild type, all other parameters analyzed were not shown to be significantly different from wild type.

Introduction

All aerobic photosynthetic carbon dioxide (CO_2) assimilation requires ribulose-1,5-bisphosphate carboxylase/oxygenase (rubisco) which is the most abundant, and arguably most important, enzyme in the world (Ellis, 1979). Rubisco can exert strong metabolic flux control over both C_3 (Hudson et al., 1992) and C_4 (von Caemmerer et al., 1997) photosynthesis. Rubisco catalyzes the first step leading to carbon fixation by binding a molecule of CO_2 to ribulose-1,5-bisphosphate (RuBP), which then forms two molecules of 3-phosphoglycerate. Then, in the presence of ATP and NADPH, these molecules are reduced to triose phosphate. Lastly, the triose

phosphate is either exported for sugar synthesis or used for RuBP regeneration for further carbon assimilation by rubisco. Rubisco has been proven to have a very slow catalytic rate relative to most enzymes, a low affinity for atmospheric CO_2, and an inefficient use of oxygen (O_2) as a substrate which leads to photorespiration. These attributes make it a seemingly inefficient enzyme for the first CO_2-fixing step of photosynthesis (Spreitzer et al., 2002). Thus, modifications to rubisco have often been discussed as an avenue to increase crop yields (Long et al., 2015; Parry et al., 2013).

The molecular mass of rubisco is large at 560 kilodaltons (kDa) and for all land plants it is composed of eight large and eight small subunits, wherein the large subunits are encoded by the chloroplast genome and the small subunits by the nuclear genome (Dean et al., 1989; Spreitzer, 1993). As of 2015, the sequences for over 150,000 large subunits and 5,000 small subunits have been deposited in GenBank. There are many barriers to modifying rubisco and also in deciding which modifications are worth testing, as genetic modifications are generally expensive and time consuming. This study examines mutations aimed at affecting the specificity of rubisco for CO_2 on its activity. Addition of a cyanobacterial bicarbonate pump to increase CO_2 concentrations ($[CO_2]$) at the site of rubisco is also examined. In this study, transformants are phenotyped to test the hypotheses that these changes increase rubisco-limited photosynthesis ($V_{c,max}$), RuBP-limited photosynthesis, net photosynthetic rate (A), and productivity relative to the control.

Materials and Methods

Plant Material

Seeds used in the following studies were obtained from Spencer Whitney from the Australian National University. Wildtype *Nicotiana tabacum* cv. Petite Havana (hereafter *N.*

tabacum), along with five transformed genotypes containing either modifications to rubisco or an addition of a bicarbonate transporter putatively affecting [CO_2] around rubisco, are compared. The MUT44 genotype carries three mutations in the rubisco large subunit, the MUT67 line codes changes in the large subunit of rubisco that impede interactions with rubisco activase, the MUT99 genotype carries a single mutation in the large subunit of rubisco, and the NL25 genotype overproduces rubisco by about 15% (Table 1). A final line was transformed to express the BicA bicarbonate transporter from *Synechococcus PCC 7942*. Transformation, composition, and confirmation of MUT44, MUT66, and MUT99 lines are described by Whitney et al. (1999) and were done using the biolistic method introduced by Svab and Maliga (1993). The BicA gene composition, transformation, and confirmation are described by Zoubenko et al. (1994) and Pengelly et al. (2014).

Field location and Experimental Design

Wild type *N. tabacum* along with the five transgenic lines were examined in the experiment were used. Seeds were started in LC-1 Sunshine Mix (SunGro Horticulture Canada Ltd, Bellevue, WA, USA) in flats in a greenhouse and thinned after germination. The field experiment was conducted at the south farms located at the University of Illinois at Urbana-Champaign (40º3'N, 88° 12'W, 228 m above sea level) during the 2013 growing season. Six weeks after germination, plants were transplanted to the field. One hundred plants per genotype were planted in 3.05 x 3.05 meter blocks at 0.3 meter spacing between each plant (Fig. 2.1). Plants were watered as necessary to maintain field capacity.

Gas Exchange

Net photosynthetic CO_2 assimilation rate was measured throughout the daylight hours 15 days after planting in the field with an open path gas exchange system equipped with a

modulated chlorophyll fluorometer (LI-6400XT, LI-COR, Lincoln, NE, USA). Measurements were made approximately every two hours from 0700 hours to 1900 hours (n=4). At each time point temperature and light levels were set according to ambient levels. Photosynthetic intercellular CO_2 response (*A/Ci*) curves were constructed in the field to determine the maximum rates of carboxylation ($V_{c,max}$), whole chain electron transport as a proxy for RuBP regeneration (J_{max}), and net photosynthetic rate (*A*) using the same gas exchange system 22 days after transplanting to the field (n=4). The gas exchange chamber CO_2 concentrations used were completed in the following order: 400, 300, 200, 100, 50, 400, 500, 600, 800 and 1000 parts per million (ppm) at 1500 µmol m^{-2} s^{-1} photosynthetically active photon flux (PPFD). $V_{c,max}$ and J_{max} values of each curve were determined using the Excel solver described by Bernacchi et al. (2003).

Leaf area and fresh leaf weight

Leaf area and fresh leaf weight was determined for each genotype (n=4) 39 days after transplanting in the field. Whole plants were selected at random and all leaves were removed to determine leaf area with an area meter (LI-3100C, LI-COR, Lincoln, NE, USA). Bulk leaves were weighed to determine fresh leaf weight.

Growth Chamber and Experimental Design

Wild type and transgenic *N. tabacum* lines were grown in controlled environments (model PCG20, Conviron, Winnipeg, Canada) in two experiments. Sample size was six for each genotype, where single plants were considered biological replicates. Seeds were planted in LC-1 Sunshine Mix (SunGro Horticulture Canada Ltd, Bellevue, WA, USA) in flats and thinned after germination. The chamber conditions were 14 hour day/10 hour nights. Day conditions were set to 300 µmol m^{-2} s^{-1} PPFD (day conditions were set to 700 µmol m^{-2} s^{-1} PPFD following

germination), 70% relative humidity, and 25˚C. Night conditions were set to 0 µmol m^{-2} s^{-1} PPFD, 70% relative humidity, and 20˚C. Two weeks after germination, plants were transplanted to 15.24 cm pots with LC-1 Sunshine Mix and 20g of Osmocote extended release fertilizer (15-9-12). Plants were watered as necessary to maintain full capacity and were rotated on a weekly basis to minimize confounding microenvironmental differences.

Gas Exchange

For the first experiment, one set of *A*/*Ci* and two sets of light response (*A/Q*) curves were measured on attached leaves beginning 39 days after planting (DAP). The CO_2 concentrations used were completed in the following order: 400, 300, 200, 100, 50, 400, 500, 600, 800 and 1000 parts per million (ppm) and 1500 µmol m^{-2} s^{-1} PPFD for the *A/Ci* curves (n=4). The first set of *A/Q* curves were measured at ambient [CO_2] (400 ppm) (n=2) and the second set were measured at elevated [CO_2] (1200 ppm) (n=2). Light levels used for both curves were 1500, 1000, 800, 500, 300, 200, 150, 100, 50, and 0 µmol m^{-2} s^{-1} PPFD. Values of $V_{c,max}$ and J_{max} of each curve were determined from the *A/Ci* curves using the Excel solver described by Bernacchi et al. (2003). *A/Q* curves were fit using a nonrectangular hyperbola described by Prioul and Chartier (1977) through use of an Excel solver developed by Lobo et al. (2013). For the second experiment, one set of *A*/*Ci* (n=4) and one set of *A/Q* (n=2) curves were measured at the aforementioned CO_2 and light levels using the LI-6400XT as previously described.

Statistical Analyses

Differences in diurnal photosynthetic rates were determined using genotype and time point as fixed effects (Proc GLM, SAS version 9.4, SAS Institute, Cary North Carolina, USA.). Differences in $V_{c,max}$, J_{max}, *A*, leaf area, and fresh weight were determined using separate linear

models and one-way ANOVAs (lm and anova, R Version 3.1.1). Significance was determined at an alpha=0.1.

In the controlled environment studies, differences in $V_{c,max}$, J_{max} and *A* were determined using separate linear models and one-way ANOVAs (lm and anova, R Version 3.1.1). Significance was determined at an alpha=0.1. Strict statistical analyses were not done on the *A/Q* curves due to low replication.

Figures and Tables

Table 2.1. Description of *N. tabacum* lines including the alteration made and the expected outcome compared to wildtype.

Line	Alteration	Expected outcome
BicA	BicA gene from *Synechococcus* PCC 7942. pRV112a derivative (Zoubenko et al., 1994; Pengelly et. al, 2014)	Increased [HCO_3^-] and [CO_2] at rubisco which should increase $V_{c,max}$ and increase A_n at all light levels and CO_2 levels.
MUT44	Three mutations in the large subunit of rubisco, pLEV1 derivative (Whitney et al., 1999)	Altered binding specificity at the site of rubisco, should make CO_2 exceedingly more preferred over O_2, increasing $V_{c,max}$ and decreasing photorespiration.
MUT67	Changes in the large subunit of rubisco that impede interactions with rubisco activase, pLEV1 derivative (Whitney et al., 1999)	Altered binding specificity at the site of rubisco, should make CO_2 exceedingly more preferred over O_2, increasing $V_{c,max}$ and decreasing photorespiration.
MUT99	Single mutation in the large subunit of rubisco, pLEV1 derivative (Whitney et al., 1999)	Altered binding specificity at the site of rubisco, should make CO_2 exceedingly more preferred over O_2, increasing $V_{c,max}$ and decreasing photorespiration.
NL25	Increased rubisco production by 15%	Increase the amount of rubisco available for carboxylation, increasing $V_{c,max}$.

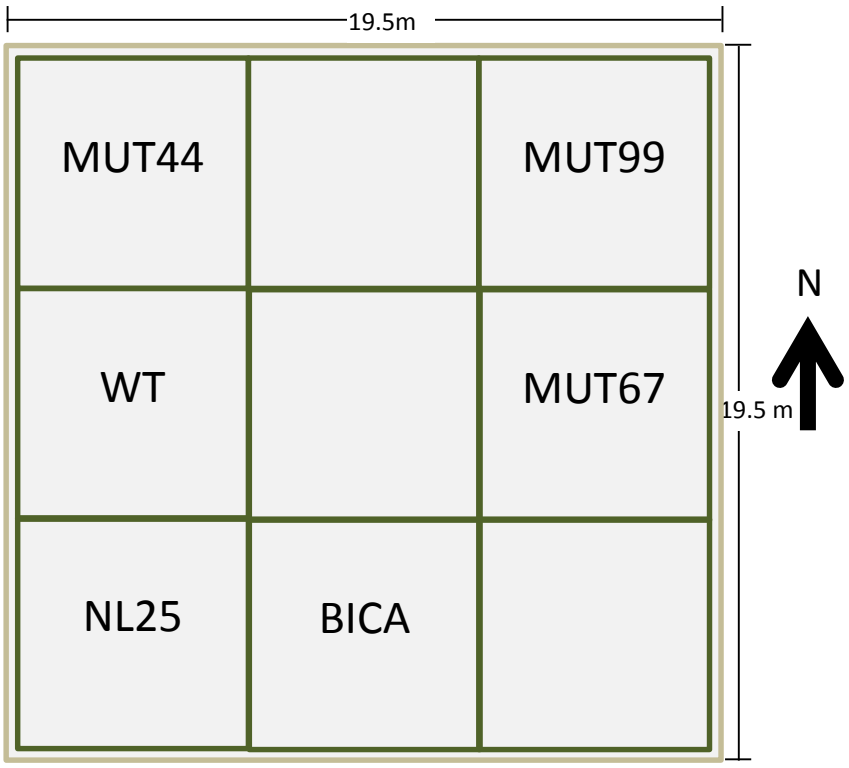

Figure 2.1. Field trial 2013 layout. n=100 per genotype. Blank boxes contain no plants.

Results

For the diurnal field measurements, there were no significant differences between genotypes within each time point (p=0.2550; Fig. 2.2). Statistical analysis showed no significant difference between genotypes for either leaf area (p=0.172; Fig. 2.3) or fresh weight (p=0.150; Fig. 2.4) at an alpha = 0.05. $V_{c,max}$ (p = 0.364; Fig. 2.5) and J_{max} (p= 0.4337; Fig 2.6) showed no significant differences between genotypes. *A* showed no significant differences between genotypes (p=0.895; Fig. 2.7).

For the first controlled environment experiment, genotypes MUT99 and NL25 were shown to have significantly lower $V_{c,max}$ values compared to wild type (p=0.0356 and p=0.0022, respectively; Fig. 2.8). There were no significant differences between J_{max} values (p=0.201; Fig. 2.9). There were no significant differences between *A* values (p=0.8113; Fig. 2.10).

For the second controlled environment experiment, genotypes MUT99 and NL25 were shown to have significantly lower $V_{c,max}$ values compared to wild type ($p<0.001$; Fig. 2.8). There were no significant differences between J_{max} values ($p=0.129$; Fig. 2.9). *A* values showed no significant differences between genotypes ($p=0.547$; Fig. 2.10). The fit data for the *A/Q* curves have also been graphed (Fig. 2.11 and 2.12).

Figures

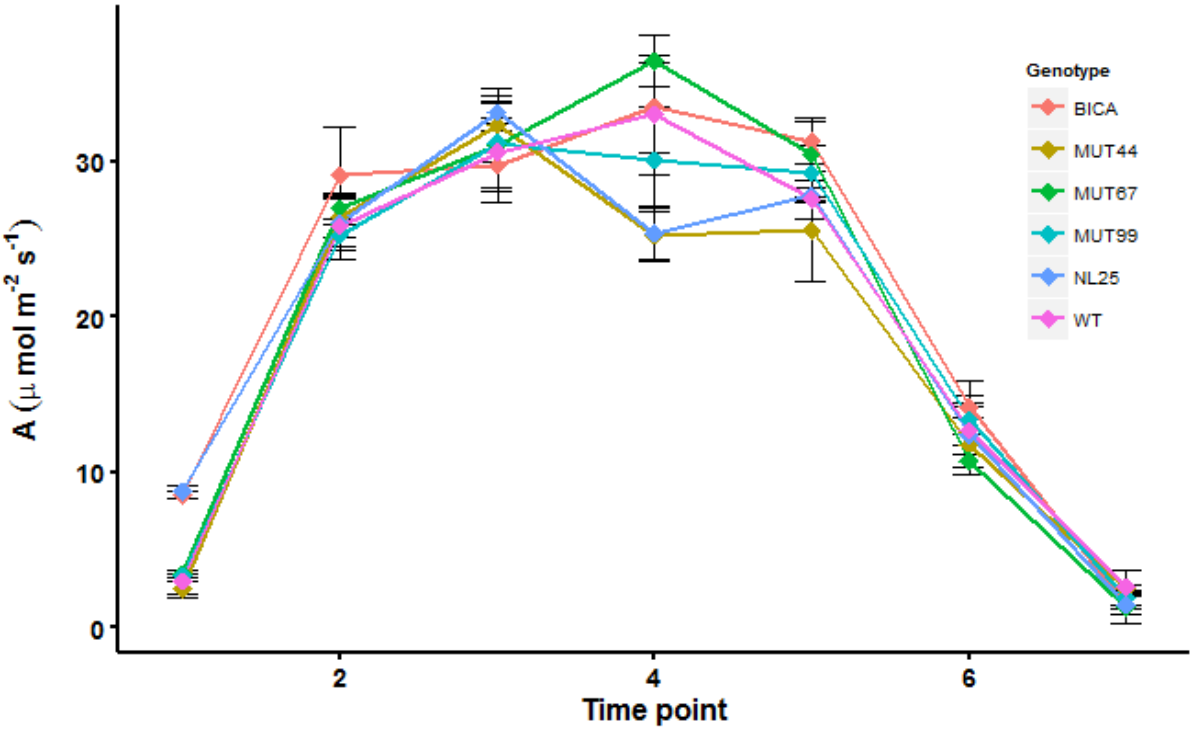

Figure 2.2. Average photosynthetic rates of each genotype at each time point compared to wild type. Bars represent ± 1 s.e. of each mean (n=4). No significant differences were found compared to wild type.

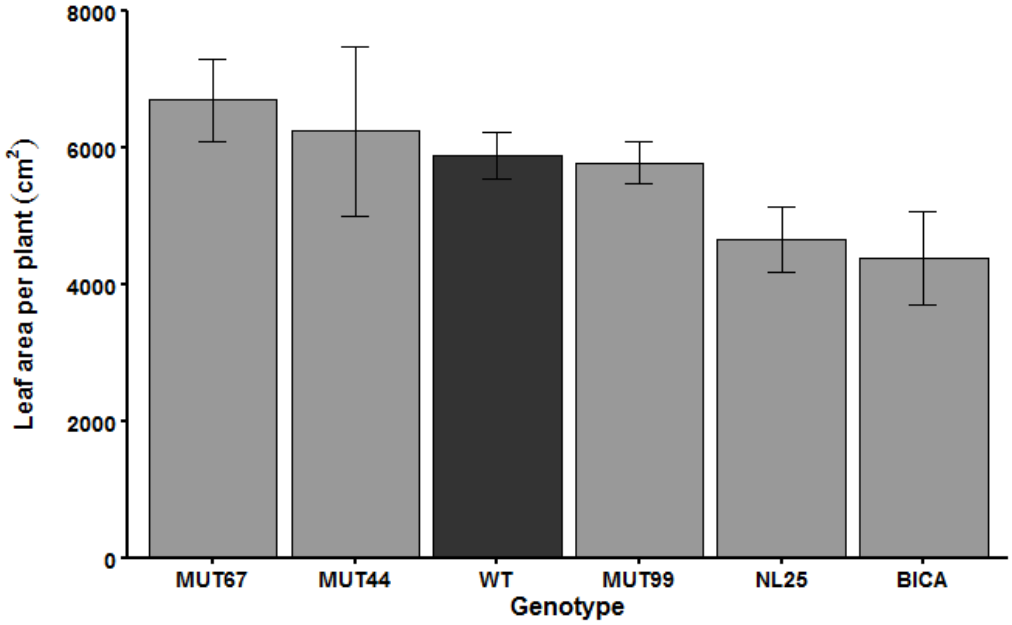

Figure 2.3. Average leaf area of each genotype expressed in cm^2. Bars represent ± 1 s.e. of each mean (n=4). No significant differences were found compared to wild type.

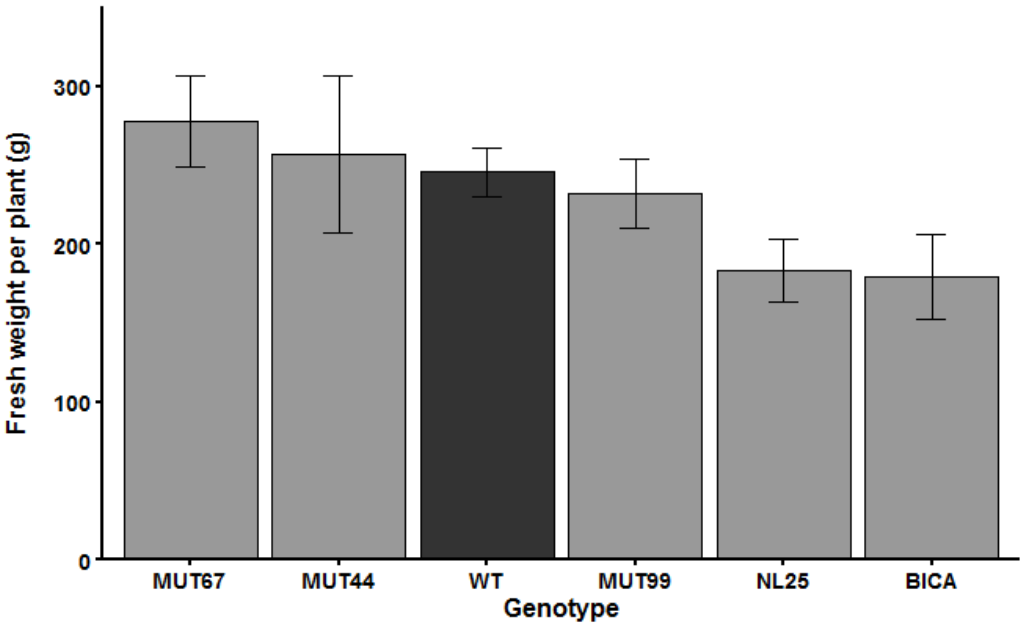

Figure 2.4. Average fresh leaf weight expressed in grams. Bars represent ± 1 s.e. of each mean (n=4). No significant differences were found compared to wild type.

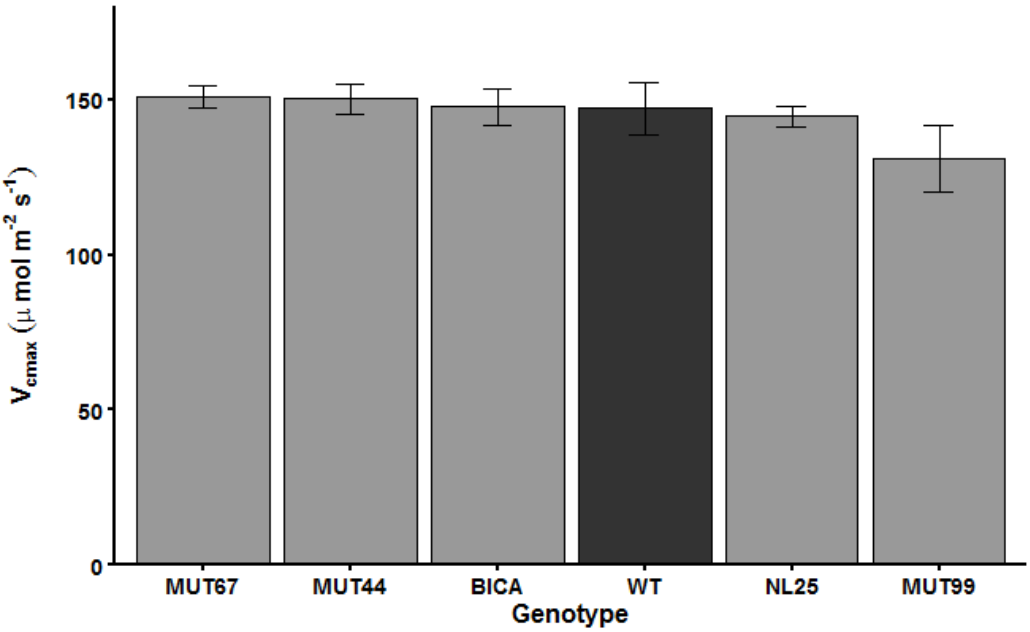

Figure 2.5. Average maximum rate of carboxylation ($V_{c,max}$) expressed in μmol$m^{-2}s^{-1}$. Bars represent ± 1 s.e. of each mean (n=4).

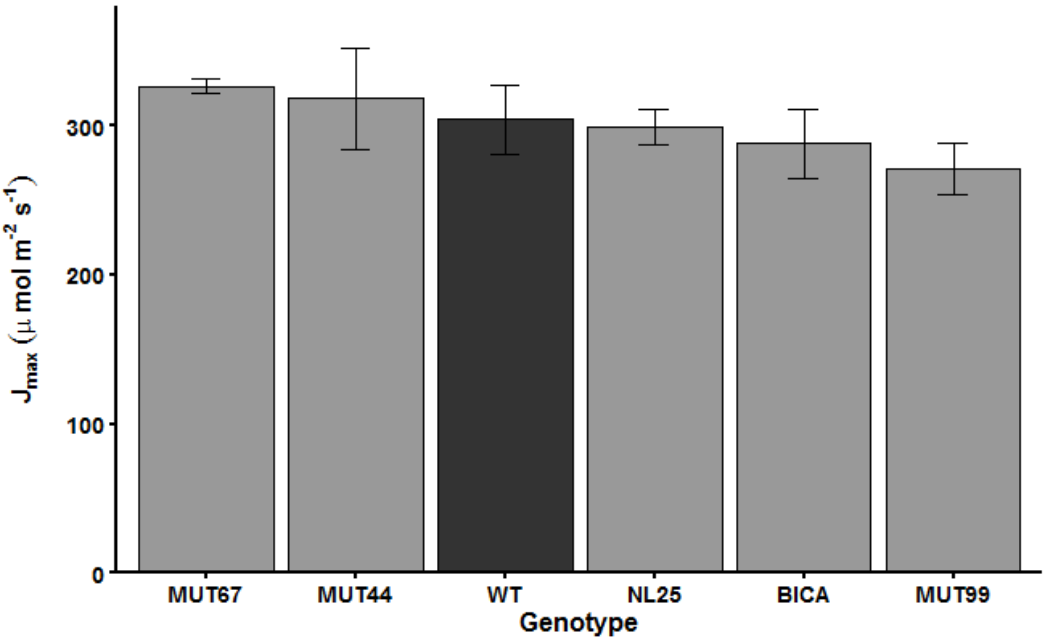

Figure 2.6. Average maximum rate of electron transport (J_{max}) expressed in μmol$m^{-2}s^{-1}$. Bars represent ± 1 s.e. of each mean (n= 4).

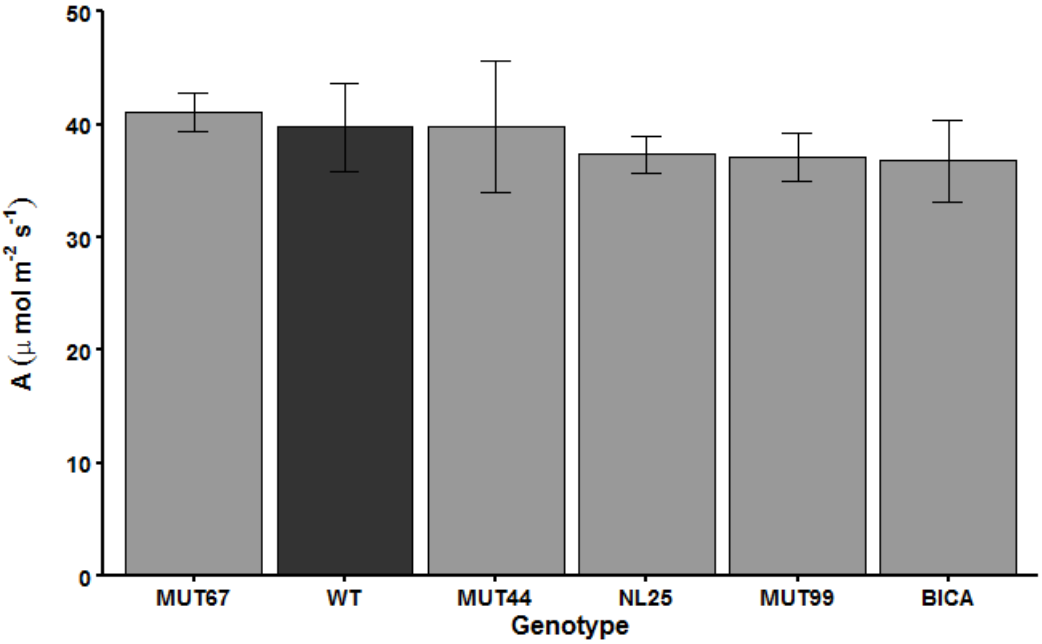

Figure 2.7. Average net photosynthetic rate (*A*) expressed in μmolm^{-2}s^{-1}. Bars represent ± 1 s.e. of each mean (n=4).

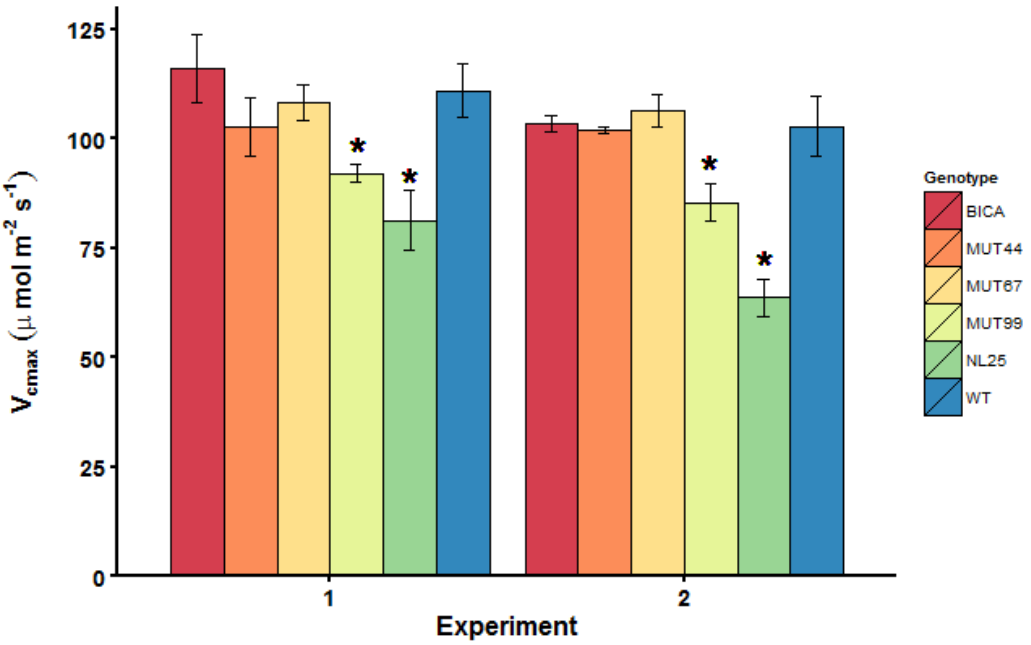

Figure 2.8. Average maximum rate of carboxylation ($V_{c,max}$) expressed in μmolm^{-2}s^{-1}. Bars represent ± 1 s.e. of each mean (n=4). Both MUT99 and NL25 on both dates showed significantly lower rates (*=p<0.001)**.**

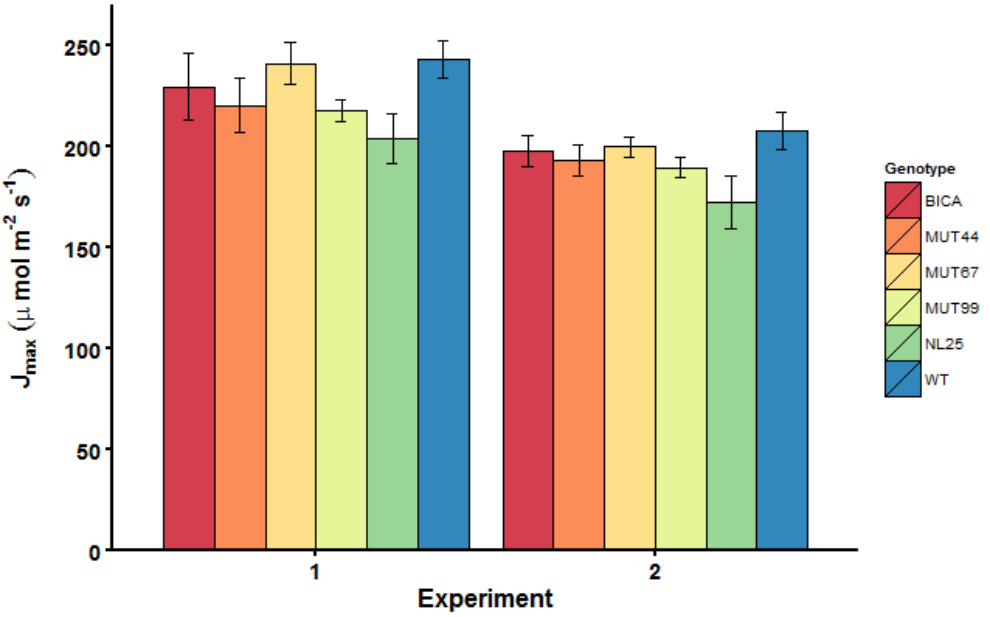

Figure 2.9. Average maximum rate of electron transport (J_{max}) expressed in μmolm^{-2}s^{-1}. Bars represent ± 1 s.e. of each mean (n=4).

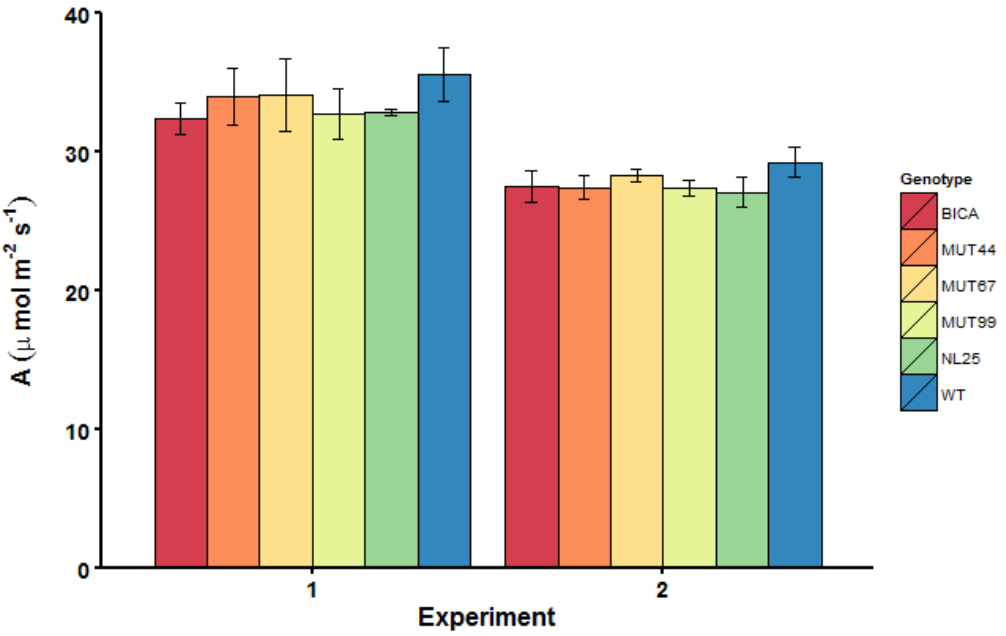

Figure 2.10. Average net photosynthetic uptake (*A*) expressed in μmolm^{-2}s^{-1}. Bars represent ± 1 s.e. of each mean (n=4).

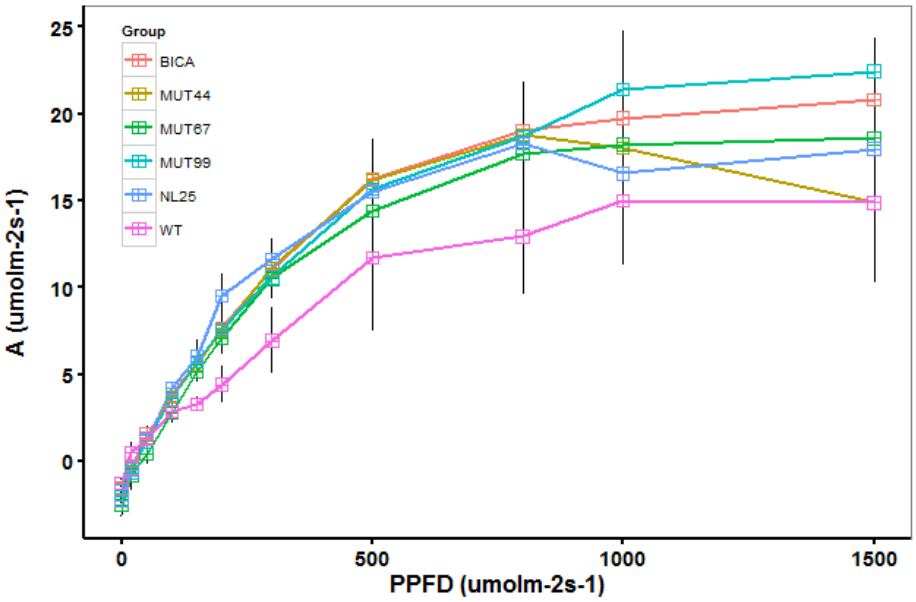

Figure 2.11. Average net photosynthetic uptake (*A*) expressed in µmolm^{-2}s^{-1} versus light level (µmolm^{-2}s^{-1}) from the first controlled environment experiment at ambient [CO_2]. Bars represent ± 1 s.e. of each mean (n=2). The colors represent the genotype.

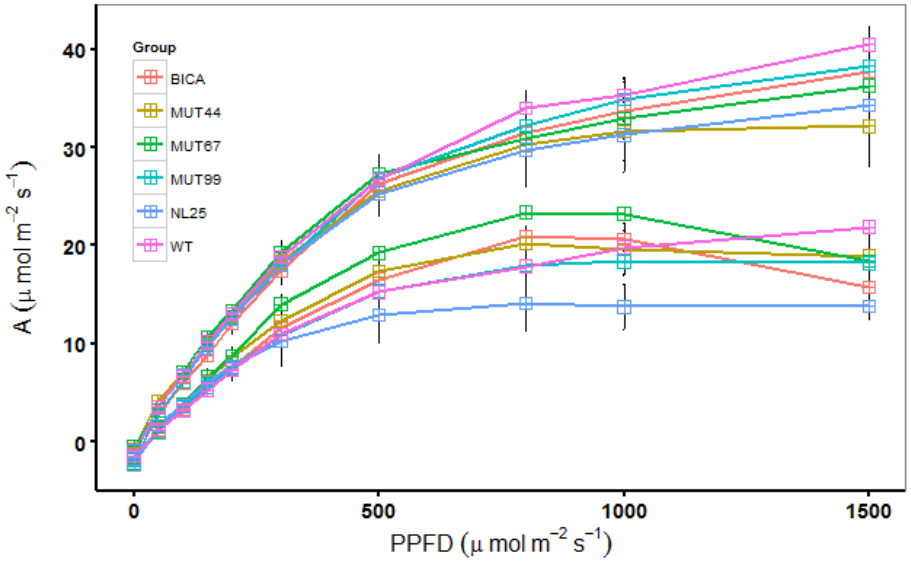

Figure 2.12. Average net photosynthetic uptake (*A*) expressed in µmolm^{-2}s^{-1} versus light level (µmolm^{-2}s^{-1}) from the second controlled environment experiment Bars represent ± 1 s.e. of each mean (n=2). The colors represent the genotype, the spatial grouping represent the [CO_2] (the upper lines are elevated [CO_2] and the lower lines are ambient [CO_2]).

Discussion

This study characterized five transformations of *N. tabacum* related to rubisco (Table 1) thought to have effects on rubisco-limited photosynthesis ($V_{c,max}$), net photosynthetic rate (*A*), and productivity due to an altered rate of photosynthetic CO_2 uptake. In the field, there were no significant differences shown in net photosynthetic uptake within each time point throughout the day, leaf area, or fresh leaf weight. In the both the first and second controlled environment experiments, there were no significant differences in RuBP-limited photosynthesis or net photosynthetic uptake, and there was significantly lower rubisco-limited photosynthesis in both NL25 and MUT99 compared to wild type.

Although the NL25 mutant overproduces Rubisco by about 15%, it has been shown that an overproduction of rubisco can lead to the inability of Rubisco activase to keep pace, which could account for lower rates of rubisco-limited photosynthesis (Crafts-Brandner and Salvucci, 2000). Additionally, if the RNA encoding the change in rubisco was not fully transcribed into DNA, it is possible that there is not the 15% increase in rubisco that is anticipated. The fine details of the change made to the binding specificity of rubiscos from MUT99 are not known, therefore it is possible that the alteration could have made the binding specificity of rubisco less sensitive to CO_2 or possibly affected rubisco binding to rubisco activase, accounting for lower levels of rubisco-limited photosynthesis. The findings related to BicA are consistent with those in the literature (Pengelly et. al, 2014). That there were no other significant differences between the transformants with altered binding specificity of rubisco and wild type indicate that the genetic modifications may have had other unforeseen effects on binding specificity or effects downstream of binding to CO_2, such as slowing the catalytic rate of the reaction due to the increase in binding specificity.

References

Crafts-Brandner, S. J., & Salvucci, M. E. (2000). Rubisco activase constrains the photosynthetic potential of leaves at high temperature and CO_2. *Proceedings of the National Academy of Sciences of the United States of America, 97*(24), 13430-13435. doi: 10.1073/pnas.230451497

Dean, C., Pichersky, E., & Dunsmuir, P. (1989). Structure, evolution, and regulation of RbcS genes in higher plants. *Annual Review of Plant Physiology and Plant Molecular Biology, 40*, 415-439.

Ellis, R. J. (1979). The most abundant protein in the world. *Trends in Biochemical Sciences, 4*(11), 241-244. doi: 10.1016/0968-0004(79)90212-3

Hudson, G. S., Evans, J. R., Voncaemmerer, S., Arvidsson, Y. B. C., & Andrews, T. J. (1992). Reduction of ribulose-1,5-bisphosphate carboxylase/oxygenase content by antisense RNA reduces photosynthesis in transgenic tobacco plants. *Plant Physiology, 98*(1), 294-302. doi: 10.1104/pp.98.1.294

Lobo, F. d. A., de Barros, M. P., Dalmagro, H. J., Dalmolin, A. C., Pereira, W. E., de Souza, E. C., . . . Rodriguez Ortiz, C. E. (2013). Fitting net photosynthetic light-response curves with Microsoft Excel - a critical look at the models. *Photosynthetica, 51*(3), 445-456. doi: 10.1007/s11099-013-0045-y

Long, S. P., Marshall-Colon, A., & Zhu, X.-G. (2015). Meeting the global food demand of the future by engineering crop photosynthesis and yield potential. *Cell, 161*(1), 56-66. doi: 10.1016/j.cell.2015.03.019

Mann, C. C. (1999). Genetic engineers aim to soup up crop photosynthesis. *Science, 283*(5400), 314-316. doi: 10.1126/science.283.5400.314

Parry, M. A. J., Andralojc, P. J., Scales, J. C., Salvucci, M. E., Carmo-Silva, A. E., Alonso, H., & Whitney, S. M. (2013). Rubisco activity and regulation as targets for crop improvement. *Journal of Experimental Botany, 64*(3), 717-730. doi: 10.1093/jxb/ers336

Pengelly, J. J. L., Foerster, B., von Caemmerer, S., Badger, M. R., Price, G. D., & Whitney, S. M. (2014). Transplastomic integration of a cyanobacterial bicarbonate transporter into tobacco chloroplasts. *Journal of Experimental Botany, 65*(12), 3071-3080. doi: 10.1093/jxb/eru156

Prioul, J. L., & Chartier, P. (1977). Partitioning of transfer and carboxylation components of intracellular resistance to photosynthetic CO_2 fixation. *Annals of Botany, 41*(174), 789-800.

Spreitzer, R. J. (1993). Genetic dissection of rubisco structure and function. *Annual Review of Plant Physiology and Plant Molecular Biology, 44*, 411-434. doi: 10.1146/annurev.pp.44.060193.002211

Spreitzer, R. J. (1999). Questions about the complexity of chloroplast ribulose-1,5-bisphosphate carboxylase/oxygenase. *Photosynthesis Research, 60*(1), 29-42. doi: 10.1023/a:1006240202051

Spreitzer, R. J., & Salvucci, M. E. (2002). Rubisco: Structure, regulatory interactions, and possibilities for a better enzyme. *Annual Review of Plant Biology, 53*, 449-475. doi: 10.1146/annurev.arplant.53.100301.135233

Svab, Z., & Maliga, P. (1993). High-frequency plastid transformation in tobacco by selection for a chimeric *aadA* gene. *Proceedings of the National Academy of Sciences of the United States of America, 90*(3), 913-917. doi: 10.1073/pnas.90.3.913

Tabita, F. R. (1999). Microbial ribulose 1,5-bisphosphate carboxylase/oxygenase: A different perspective. *Photosynthesis Research, 60*(1), 1-28. doi: 10.1023/a:1006211417981

von Caemmerer, S., Millgate, A., Farquhar, G. D., & Furbank, R. T. (1997). Reduction of ribulose-1,5-bisphosphate carboxylase/oxygenase by antisense RNA in the C-4 plant *Flaveria bidentis* leads to reduced assimilation rates and increased carbon isotope discrimination. *Plant Physiology, 113*(2), 469-477.

Whitney, S. M., von Caemmerer, S., Hudson, G. S., & Andrews, T. J. (1999). Directed mutation of the Rubisco large subunit of tobacco influences photorespiration and growth. *Plant Physiology, 121*(2), 579-588. doi: 10.1104/pp.121.2.579

Zoubenko, O. V., Allison, L. A., Svab, Z., & Maliga, P. (1994). Efficient targeting of foreign genes into the tobacco plastid genome. *Nucleic Acids Research, 22*(19), 3819-3824. doi: 10.1093/nar/22.19.3819

CHAPTER 3: ASSESSING THE EFFECTS OF CYANOBACTERIAL GENE EXPRESSION, *ICTB* AND *SBFB,* INTRODUCED INTO *GLYCINE MAX* CV. THORNE

Abstract

Because cyanobacteria have a unique way of concentrating carbon dioxide around rubisco, they can perform photosynthesis more efficiently than land plants performing C_3 photosynthesis. Two different cyanobacterial genes predicted to enhance photosynthetic conversion efficiency, *ictB* and *SBFB,* were independently engineered into *Glycine max* cv. Thorne. Plants were grown in two controlled environment experiments and one agricultural field experiment in 2014. Leaf carbon dioxide uptake rates and responses to changes in intercellular carbon dioxide were determined and analyzed. Final harvest metrics were also collected and analyzed. Total average seed yields for one of the *ictB* events (C) and *SBFB* were shown to have 45% and 75% of the yield compared to wild type, respectively.

Introduction

Cyanobacteria have the ability to concentrate carbon dioxide (CO_2) around the site of rubisco due to specialized CO_2 channels and a structure called a carboxysome. The carboxysome is an icosahedral structure that has rubisco and carbonic anhydrase bound to its interior walls. Bicarbonate is actively transported from the environment into the cytosol of the cyanobacteria, while CO_2 is hydrated to bicarbonate by NADH. Once inside the carboxysome, the carbonic anyhdrase is quickly converted to CO_2 by bicarbonate, allowing for high concentrations of CO_2 around rubisco and competitive inhibition of the oxygenase reaction (Badger and Price, 2003). A putative dissolved inorganic carbon transporter, *ictB,* from the cyanobacterium *Synchococcus PCC 7942* (Bonfil et al., 1998) has been engineered into *Arabidopsis thaliana* and *Nicotiana tabacum,* which resulted in increased productivity, increased photosynthesis, a lower

photosynthetic carbon dioxide concentration compensation point, and increased water use efficiency (WUE; defined as the ratio of carbon dioxide assimilation to transpiration) (Liemean-Hurwitz et al., 2003). An additional study that investigated a previous generation (T3) of the same transformation used in this study showed a 10% increase in the *in vivo* rate of RuBP-limited photosynthesis, a 9% increase in RuBP-saturated photosynthesis, 13% increase in final plant mass and 15% increase in seed yield in one event (4746-4) in an controlled environment chamber (Hay, 2012). Hay also found a 15% increase in leaf carbon uptake in a two year field trial. These findings point to decreased photorespiration, which is associated with a higher CO_2 concentration at the site of rubisco. However, the T4 generation of these transformations were also analyzed in a field trial in 2012 and it was found that there were no significant increases in the same parameters compared in 2010 and 2011 between *ictB* and the control. In fact, significant decreases in yield were observed, though it was considered a drought year (Bishop, unpublished).

IctB was first identified from a knockout mutant of *Synechococcus* that could only grow normally in a high carbon dioxide environment (5% v/v), indicative of a loss of CO_2-concentrating function. The encoded protein contains 10 transmembrane regions, is inner-membrane located, and was putatively classified as a bicarbonate transporter (Bonfil et al,. 1998). In wild type cells, there is a correlation between the presence of sodium ion-dependent bicarbonate uptake and the accumulation of the *ictB* protein (Amoroso et al., 2003). Contrarily, a quadruple bicarbonate transporter knockout mutant of *Synechocystis PCC 6803* was created that showed no transport activity, even with a homolog (*Slr1515*) of *ictB* present (Shibata et al., 2002). Thus, although knockouts of *ictB* expression have shown that it is essential to bicarbonate uptake in *Synechocytis* (Price et al., 2011) and the engineering of *ictB* into two higher plants

showed increased photosynthetic uptake, the previous studies evaluating these specific soybean lines have not produced consistent results, which make the alteration interesting to explore further.

The expression of the cyanobacterial gene that encodes for the bifunctional enzyme fructose-1,6-bisphosphate/sedoheptulose-bisphosphatase (*SBFB*) in higher plants is also an avenue for enhanced photosynthetic efficiency in C_3 crops. This bifunctional enzyme performs the combined function of the two individual enzymes found in higher plants, fructose-1,6-bisphosphate (FBPase) and sedoheptulose-bisphosphatase (SBPase). These two enzymes regulate steps in the reductive pentose-phosphate (Calvin) cycle, which is the primary carbon fixation pathway in higher plants (Sharkey, 1985). They partly compose the reactions responsible for the regeneration of ribulose-1,5-bisphosphate (RuBP) for continued use by rubisco for carbon assimilation. Systems modeling of light-saturated photosynthesis suggests that both SBPase and FBPase exert strong metabolic control (Zhu et al. 2007). These enzymes influence the point at which photosynthesis becomes RuBP-limited, which occurs when RuBP regeneration can no longer supply the demand of RuBP needed to initiate increased levels of photosynthesis. Transgenic tobacco plants over-expressing a plant SBPase were shown to have enhanced yields due to greater light-saturated photosynthetic rates and accelerated growth, leading to increases in leaf area and biomass by up to 30% (Lefebvre et al., 2005). Transgenic tobacco plants over-expressing a chloroplast-targeted FBPase/SBPase bifunctional cyanobacterial enzyme also showed a 24% increase in final dry matter and 50% increase in photosynthetic carbon dioxide fixation (Miyagaea et al., 2001).

In this study, *Glycine max* cv. Thorne (hereafter *G. Max*) plants expressing the *ictB* gene and others expressing the *SBFB* gene were phenotyped to assess the prediction that the

expression of the *ictB* gene will have increased rates of Rubisco-limited photosynthesis and RuBP regeneration-limited photosynthesis and the prediction that the expression of the *SBFB* gene will have increased rates of RuBP regeneration-limited photosynthesis.

Materials and Methods

Plant Material

Seeds used in this experiment were originally obtained from Tom Clemente at the University of Nebraska. At Nebraska, seeds of *G. max* cv. Thorne were transformed with the cyanobacterial gene *ictB* under the control of the 35S CaMV promoter combined with the pea SSU transit peptide to facilitate transport across the plastid membrane (Fig. 3.1). Three separate events of *ictB* transformed *G. max* were examined, 474-6 (A), 468-7 (B), and 474-1 (C). An additional transformation, referred to in this study as *SBFB*, was transformed with the cyanobacterial gene that encodes for an FBPase/SBPase bifunctional enzyme (Fig. 3.2). All were provided as putatively homozygous T2 lines. Both the *ictB* and *SBFB* transformation events included the bar gene to confer glufosinate ammonium resistance as a selectable marker. Previous studies in 2010 and 2011 examined the 474-6 (A) and *SBFB* event (Hay, 2012), in 2012 all three *ictB* lines were examined (Bishop, unpublished). Wild type, *ictB* lines, and the *SBFB* line were all grown using seeds from the same populations of the studies performed from 2010-2012. Thus, the seeds used are, at minimum, from the fifth generation (T5).

Verification of ictB mRNA

Leaf discs (50.3 mm^2) for mRNA expression verification were collected from plants of the same generation grown in a greenhouse on DOY 126 prior to the beginning of this field experiment. Ten leaf disks per leaf were taken and immediately frozen in liquid nitrogen and stored at -80˚C. RNA was extracted using the Qiagen RNAeasy RNA extraction kit. The Life

Technologies SuperScript III First-Strand Synthesis System for RT-PCR was used to produce cDNA. These products were combined with Life Technologies Platinum Taq DNA Polymerase and custom primers for *ictB*. The mixture was then put in a thermocycler and incubated using a protocol optimized for SuperScript cDNA and Platinum Taq Polymerase. The products of this reaction were run on an ethidium bromide-stained gel and viewed under UV-light for confirmation of *ictB* mRNA presence. Verification of *SBFB* mRNA was not done because it was confirmed to be expressed on the level of mRNA (Clemente, personal communication).

Growth Chamber and Experimental Design

Wild type *G. max*, the three events of *G. max* transformed with the *ictB* gene, and one event of *G. max* transformed with *SBFB* gene were grown in a controlled environment (model PCG20, Conviron, Winnipeg, Canada) in two separate experiments. Sample size was five for each of the four events and for the wild type where single plants were considered biological replicates. Four seeds per genotype were planted in LC-1 Sunshine Mix (SunGro Horticulture Canada Ltd, Bellevue, WA, USA) contained in 7.6 liter pots and thinned to one plant per pot after emergence. The chamber conditions were 14 hour days and 10 hour nights. Day conditions were set to 750 µmol m^{-2} s^{-1} PPFD, 65% relative humidity, and 25˚C. Night conditions were set to 0 µmol m^{-2} s^{-1} PPFD, 65% relative humidity, and 22˚C. After one week of emergence, plants were fertilized with 50% Long-Ashton nutrient solution every other day. Plants were also rotated on a weekly basis to avoid microenvironmental differences with between sample and genotype differences.

Gas exchange

In the first experiment, two sets of *A/Ci* curves and net photosynthetic CO_2 uptake (*A*) were measured on attached leaves using an open path gas exchange system equipped with a

modulated chlorophyll fluorometer (LI-6400XT, LI-COR, Lincoln, NE, USA) on the central leaflet from the youngest, fully expanded, trifoliate of each plant. Photosynthesis was induced at 400 ppm [CO_2] and 1500 µmo lm^{-2} s^{-1} PPFD 34 days after planting (DAP). The *A/Ci* curves were performed approximately 2 weeks apart, the first set taking place 37 DAP and the second set 52 DAP. The CO_2 concentrations used were completed in the following order: 400, 300, 200, 100, 50, 400, 600, 800, 1200 and 1500 ppm at 1000 µmol m^{-2} s^{-1} PPFD, following the procedure of Long & Bernacchi (2003). *A/Ci* curves were analyzed using the Excel solver developed by Bernacchi et al. (2003) to determine the maximum carboxylation capacity of Rubisco ($V_{c,max}$) and the maximum rate of electron transport (J_{max}). For the second experiment, *A/Ci* curves were performed 26 DAP and *A/Q* curves were performed 27 DAP. The light levels used for the *A/Q* curves were 250, 200, 150, 100, 75, 50 and 25 µmol m^{-2} s^{-1} PPFD. Light levels were changed when the attached leaf was no longer experiencing large fluctuations in conductance and photosynthesis. Harvest Index and seed yield for each individual plant were also determined for the first experiment. The total number of seeds per plant was estimated by weighing ten seeds selected at random, taking the average, and dividing the total weight by that average.

Field Location and Experimental Design

The study was conducted on the University of Illinois Urbana-Champaign's Energy Farm located in Urbana, Illinois in 2014. In this study, seeds were sown in a completely randomized design (n=4 plots) of each genotype for a total of 20 plots in ambient field conditions on day of year (DOY) 150 (Experimental outline, Table 3.1). Each plot contained three rows, 2.5 meters in length, with 0.762 meter row spacing (common for Illinois planting) and 5.08 centimeters between each plant for 20 plants per linear meter, or 106,000 seeds/acre. The planting density chosen was slightly less dense than what is normally planted in the area, but was chosen due to

seed availability. The border of the entire 10 m x 11.43 m plot was surrounded by two wild type-planted rows as required by the APHIS permit (Fig. 3.3).

Gas exchange

For photosynthetic measurements, shoots of *G. max* were cut at the base pre-dawn and again cut underwater to prevent embolism. These shoots were then transferred to a laboratory where the shoots were allowed to acclimate for at least thirty minutes under 500 µmol m^{-2} s^{-1} PPFD. *A/Ci* curves were measured on the most recently expanded trifoliate on the mainstem. Measurements were made on DOY182-183, 204-205, and 226-227 and were analyzed using the protocol of Bernacchi et al. (2003). Measurements were taken at 25ºC, 1500-1750 µmol m^{-2} s^{-1} PPFD, and CO_2 concentrations of The CO_2 concentrations used were completed in the following order: 400, 300, 200, 100, 50, 400, 600, 800, 1200 and 1500 ppm using a LI-COR 6400XT. An average of 4 plants per plot were analyzed during each measuring period.

Glufosinate ammonium painting

On DOY 232 and 233 a portion of a leaf of every plant of every plot was painted with a solution of glufosinate ammonium and marked with a permanent marker to denote where the herbicide was applied. Leaves were monitored for 2 weeks to determine resistance to the herbicide to confirm presence of the transgene. If plants did not show chlorosis at the marker line, they were determined to be resistant.

Final Harvest

Plants were harvested from the field on DOY 273, 274, and 279. They were allowed to air dry for two days before being weighed and threshed. Harvest index was determined by separating the pods from stems by hand from the middle rows (each 2.5 m in length) from each

of the 20 plots. Stem and pod biomass were weighed and pods mechanically threshed. Harvest index was determined by dividing seed biomass over total biomass for each 2.5m.

Yield was determined by taking the remaining 2 rows (totaling 5 m in length per plot) from each of the 20 plots. Each whole plant was mechanically threshed and yield was determined by weighing the seeds from each plot.

Statistical Analysis

Controlled environment experiments were analyzed separately from each other. For the first controlled environment experiment, differences in $V_{c,max}$, $J_{max,}$ and *A* were determined using a repeated measures complete mixed model analysis of variance (PROC MIXED, SAS 9.4; SAS Institute, Cary, N.C.) with genotype as a fixed effect. For the second environment controlled experiment, differences in $V_{c,max}$, $J_{max,}$ *A,* and final harvest metrics were determined through use of independent simple linear models (lm, R Version 3.1.1). For the field trial, differences in $V_{c,max}$, J_{max}, and *A* were determined using a repeated measures complete mixed model analysis of variance (PROC MIXED, SAS 9.4; SAS Institute, Cary, N.C.) with genotype as a fixed effect. Differences in the final harvest metrics were determined through use of independent simple linear models (lm, R Version 3.1.1). Significant differences for each test was determined at an alpha=0.1. No formal statistical tests were used on the *A/Q* curves due to low replication.

Figures and Tables

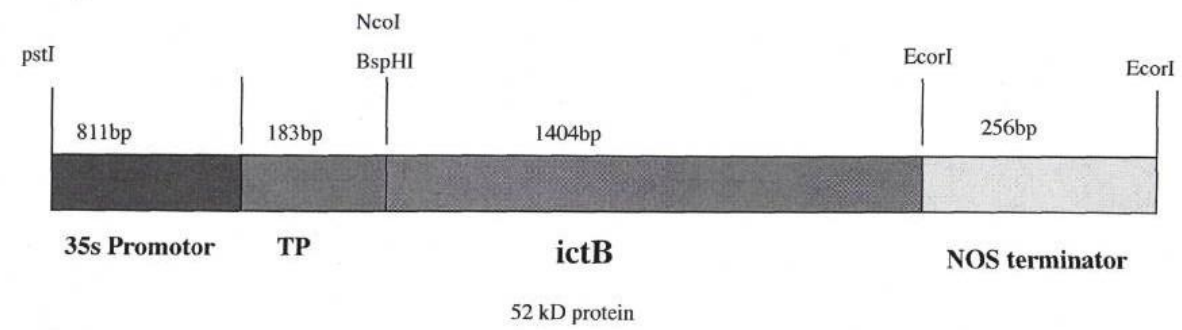

Figure 3.1. *IctB* gene construct used in the agrobacterium-mediated transformation of *Glycine max* cv. *Thorne*. The *ictB* gene of interest is under the control of the 35S CaMV promoter, and is coupled to the pea SSU transit peptide for transport across the plastid membrane. (Hay, 2012)

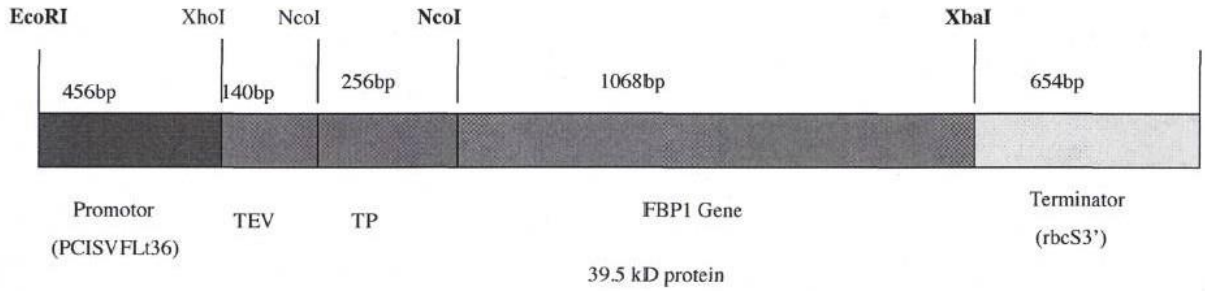

Figure 3.2. *FBP1* gene construct used in the agrobacterium-mediated transformation of *Glycine max* cv. Thorne. The *FBP1* gene of interest is under the control of the peanut chlorotic streak virus promoter, coupled with the tobacco etch translational enhancer element. Note: *FBP1* referred to as *SBFB* in this study. (Hay, 2012)

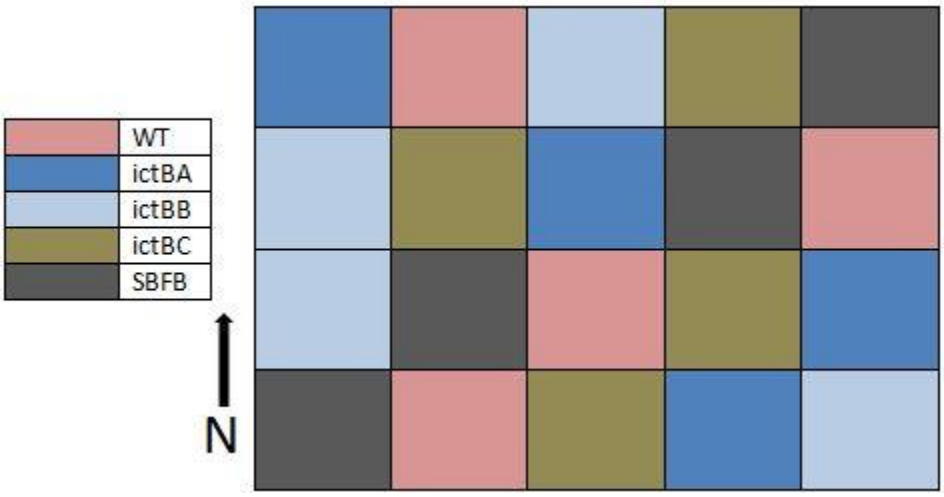

Figure 3.3. Field layout for May 2014 field experiment. Each colored box represents one plot. N indicates north. Dimensions are 14.5m x 12m.

Table 3.1. Table outlining the growth stages and measurements taken in the experimental plot on a given day.

Date	Day of year	Growth stage	Measurement taken
30 May 2014	150	Seeds sown	
5 June 2014	156	Plants emerge	
1 July 2014	182	WT, A, B, *SBFB*: V5 C: V4	*A/Ci* curves
23 July 2014	204	Beginning flowering	*A/Ci* curves
14 August 2014	226	Beginning seed	*A/Ci* curves
20 August 2014	232	Beginning seed	*BASTA* painting
30 September 2014	273	Full maturity	Harvest

Results

The presence of *ictB* mRNA transcripts were shown to be present for all transformants of the A, B, and C lines and were not present for the wild type control (Fig.3.4). Because mRNA was confirmed to be expressed, the lines were used for further study.

For the first controlled environment experiment there were no significant differences within each date for $V_{c,max}$ ($p=0.27$; Fig. 3.5) and *A* ($p=0.3$; Fig. 3.6). For J_{max}, the model was significant ($p=0.07$), however a Tukey's test revealed no significant differences compared to

wildtype (Fig. 3.7). For the second environment controlled experiment, there were no significant differences for $V_{c,max}$ (p=0.949; Fig. 3.8), J_{max} (p=0.99; Fig. 3.9), *A* (p=0.920; Fig. 3.10) compared to wild type. Additionally, there were no significant differences between seed yield (p=0.535; Fig. 3.11), pod weight (p=0.528; Fig. 3.12), total seed number (p=0.259; Fig. 3.13), or the ratio of seed weight to pod + seed weight (p=0.43; Fig. 3.14). Fit *A/Q* curves have also been graphed, along with the average maximum quantum yield of each line ($\Phi_{CO2,max}$) (Fig. 3.15).

For the field experiment the models for $V_{c,max}$ (p=0.07; Fig. 3.16) and J_{max} (p=0.08; Fig. 3.17) were significant, however, a post hoc Tukey's test revealed no significant differences compared to wild type. There were no significant differences observed within dates for *A* (p=0.11; Fig. 3.18). Lines A, B, C, and *SBFB* showed glufosinate ammonium resistance, indicating the presence of the resistance gene. Total average seed yields for one event of the *ictB* transformation and the *SBFB* transformation showed significantly lower yields at an average of 45% and 75% of wild type, respectively (p=0.000005 and p=0.0032, respectively; Fig. 3.19). However, there were no significant differences in harvest index (p=0.551; Fig. 3.20).

Figures

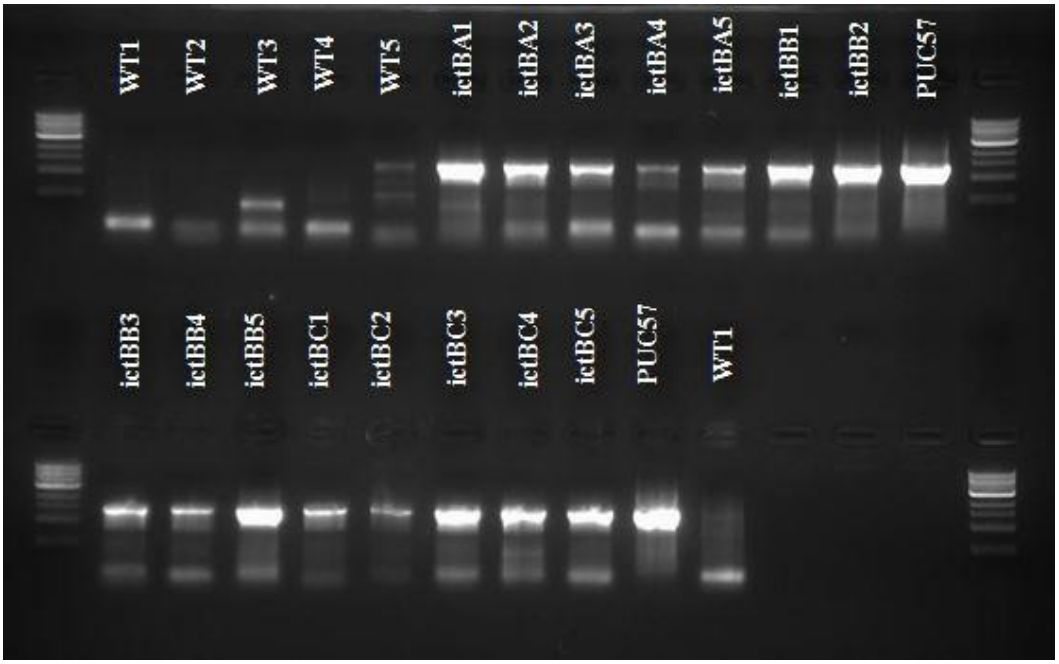

Figure 3.4. Ethidium bromide-stained gel under UV light. Each well represents a different plant from each respective line. PUC57 refers to a vector already confirmed to have the *ictB* gene present. A band at 1400 bp confirms *ictB* presence.

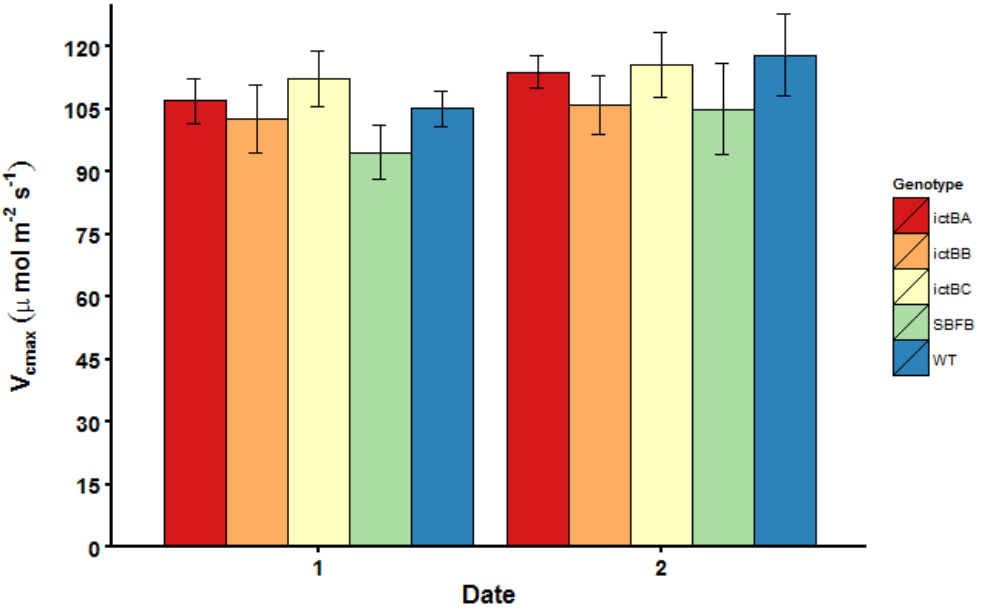

Figure 3.5. Average maximum rate of carboxylation ($V_{c,max}$) expressed in μmol$m^{-2}s^{-1}$. Date 1 and 2 refer to 37 and 52 DAP in the first experiment. Bars represent ± 1 s.e. of each mean (n=5).

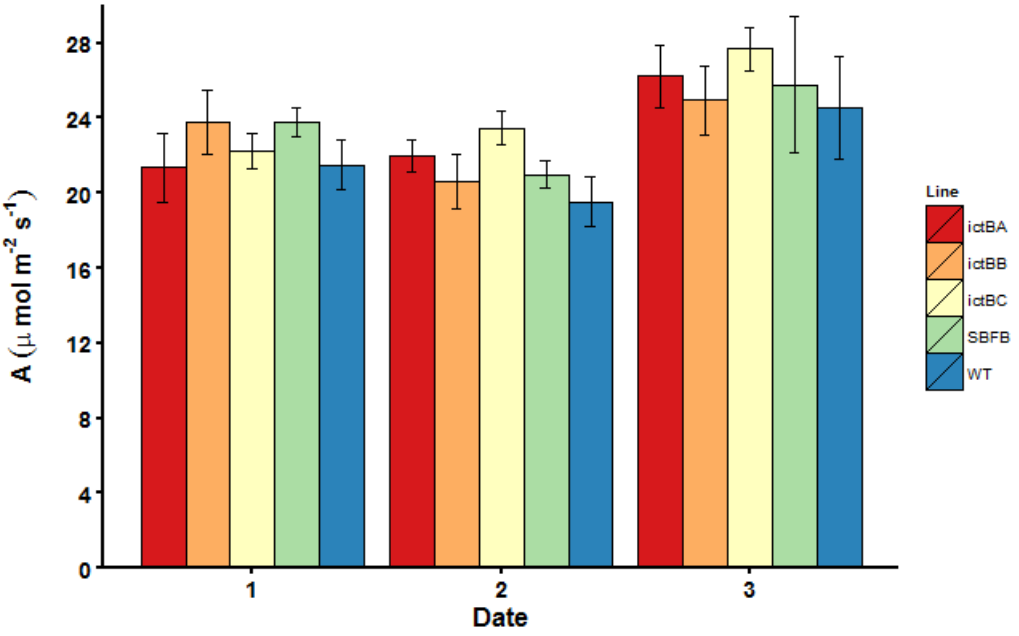

Figure 3.6. Average net photosynthetic uptake (*A*) expressed in μmolm^{-2}s^{-1} Date 1, 2, and 3 refer to 34, 37, and 52 DAP, respectively, in the first experiment. Bars represent ± 1 s.e. of each mean (n=5).

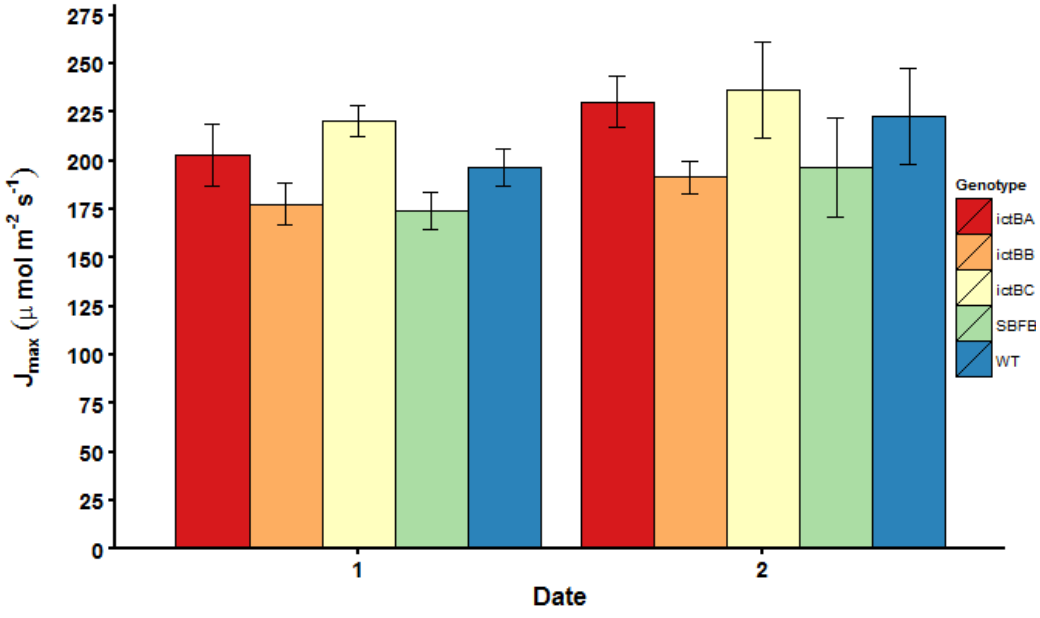

Figure 3.7. Average maximum rate of electron transport (J_{max}) expressed in μmolm^{-2}s^{-1}. Date 1 and 2 refer to 37 and 52 DAP, respectively, in the first experiment. Bars represent ± 1 s.e. of each mean (n=5).

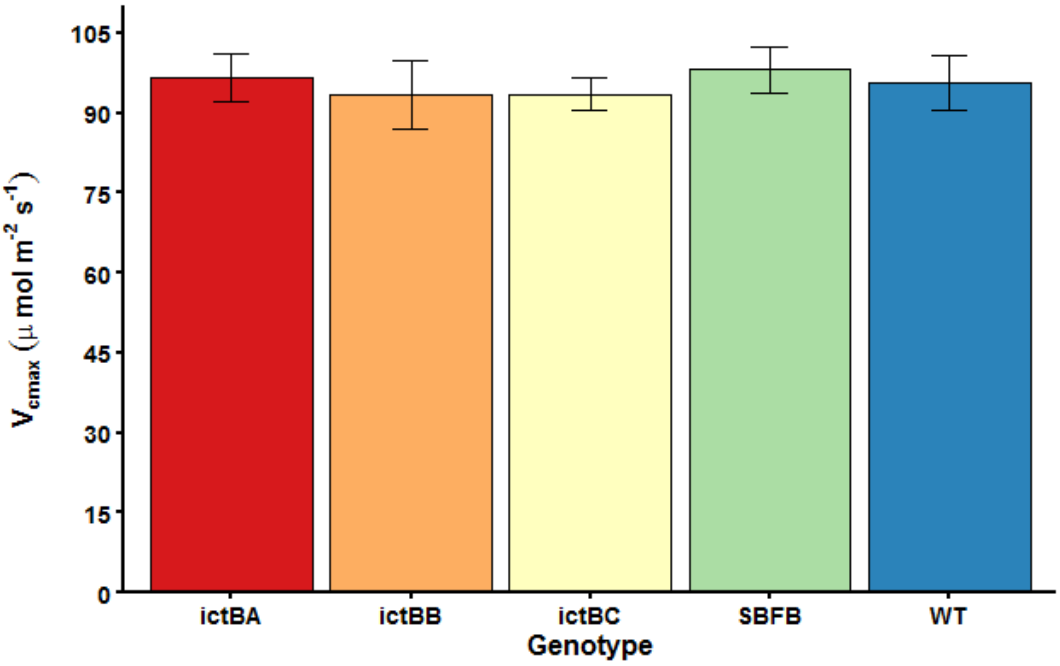

Figure 3.8. Average maximum rate of carboxylation ($V_{c,max}$) expressed in μmol$m^{-2}s^{-1}$ for the second experiment. Bars represent ± 1 s.e. of each mean (n=5).

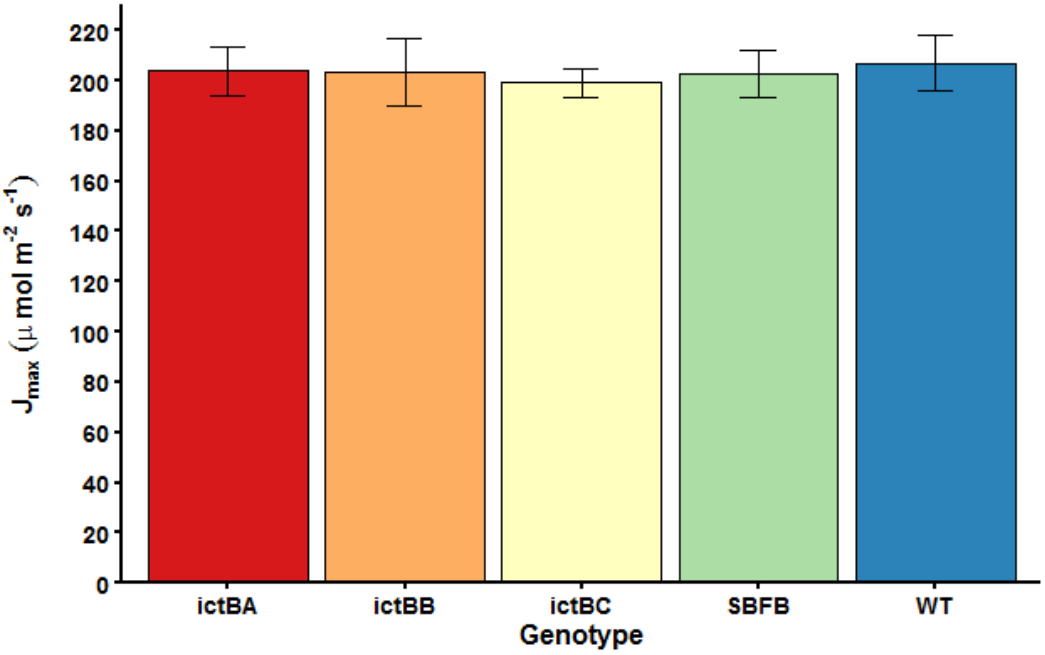

Figure 3.9. Average maximum rate of electron transport (J_{max}) expressed in μmol$m^{-2}s^{-1}$ for the second experiment. Bars represent ± 1 s.e. of each mean (n=5).

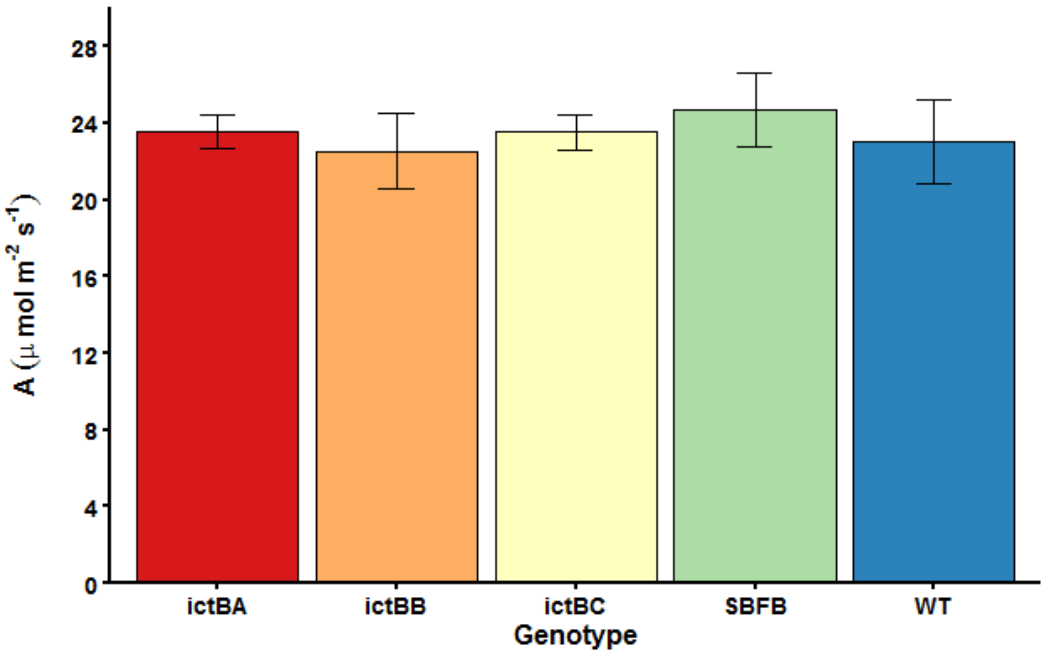

Figure 3.10. Average net photosynthetic rate (A) expressed in μmolm^{-2}s^{-1} for the second experiment. Bars represent ± 1 s.e. of each mean (n=5).

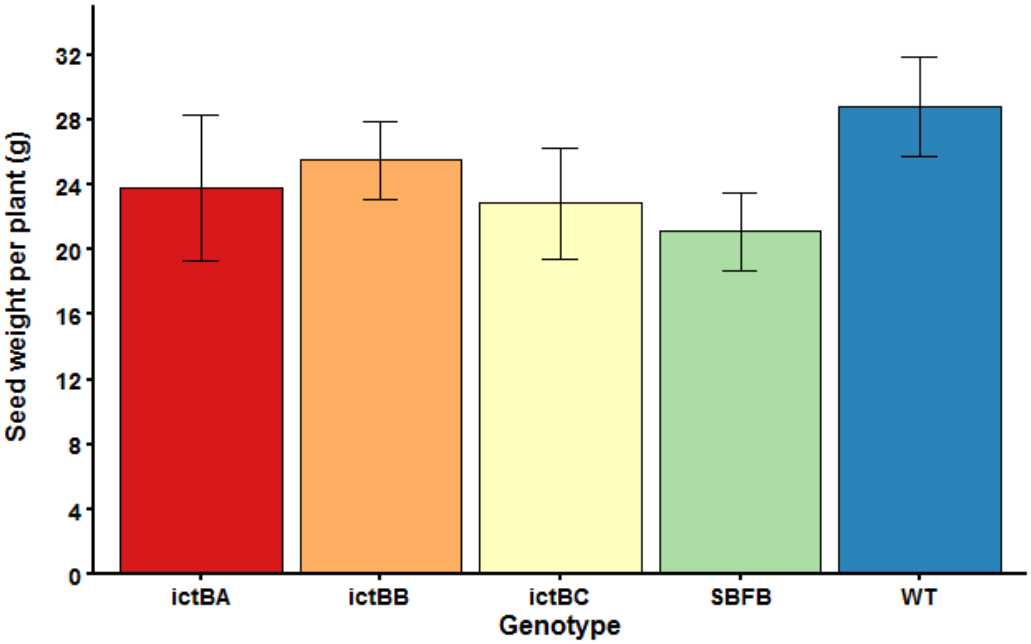

Figure 3.11. Average seed weight per plant in grams for the second experiment. Bars represent ± 1 s.e. of each mean (n=5).

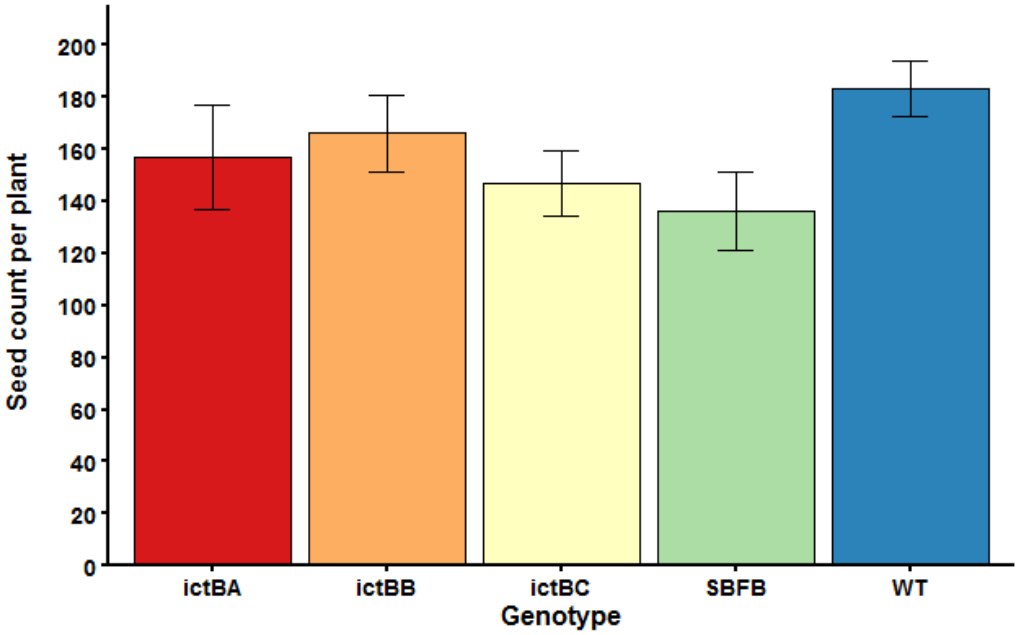

Figure 3.12. Average pod weight per plant for the second experiment. Bars represent ± 1 s.e. of each mean (n=5).

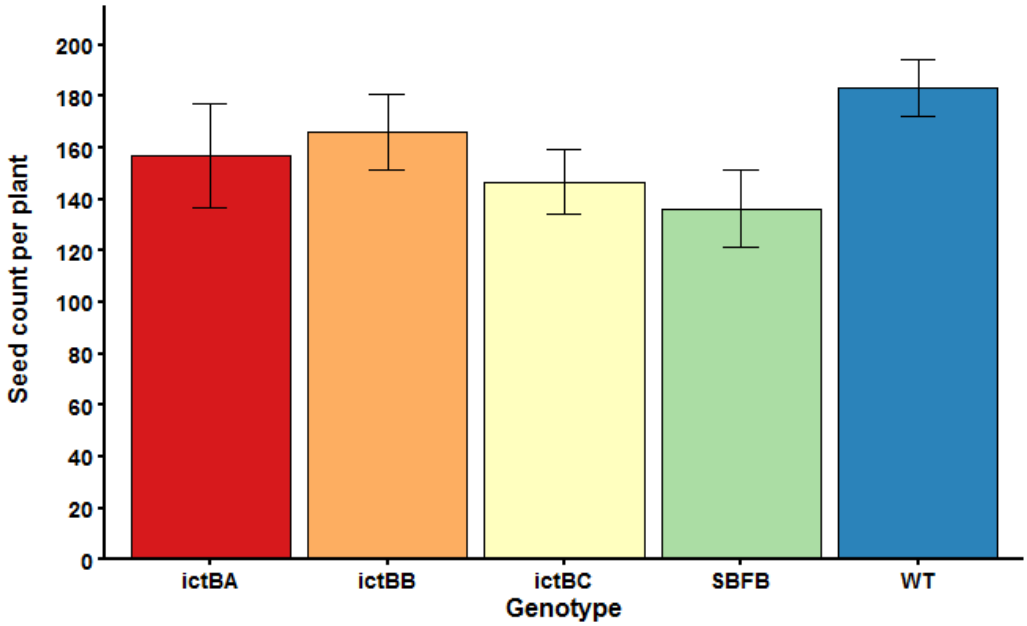

Figure 3.13. Average seed count per plant for the second experiment. Bars represent ± 1 s.e. of each mean (n=5).

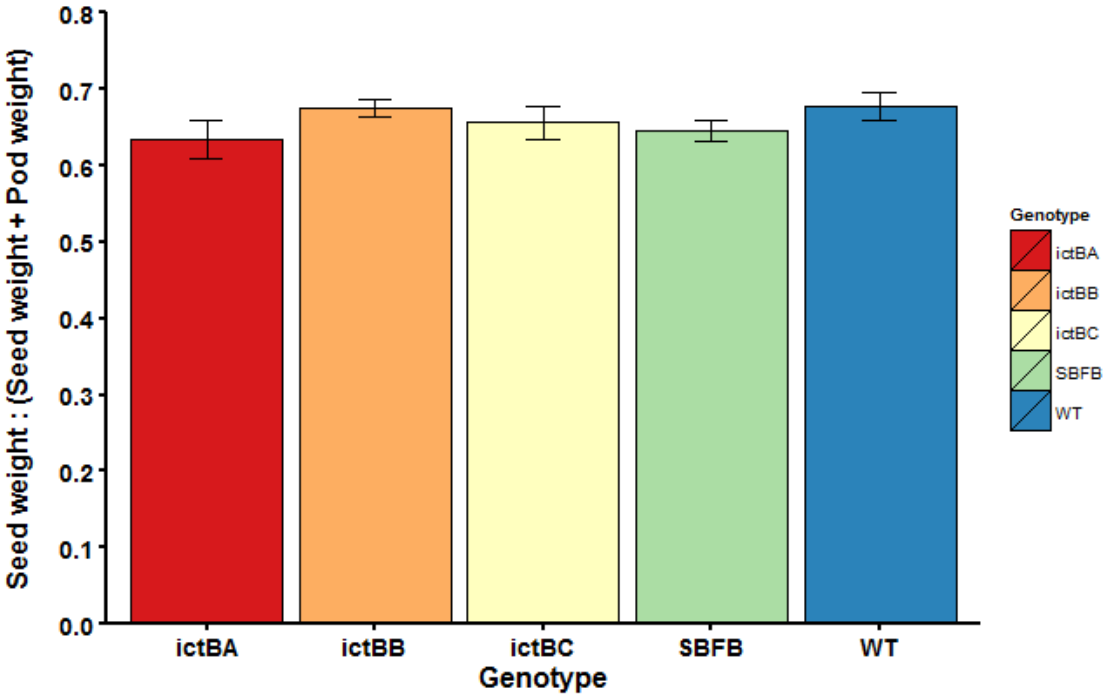

Figure 3.14. Average seed weight : (seed weight + pod weight) ratio for the second experiment. Bars represent ± 1 s.e. of each mean (n=5).

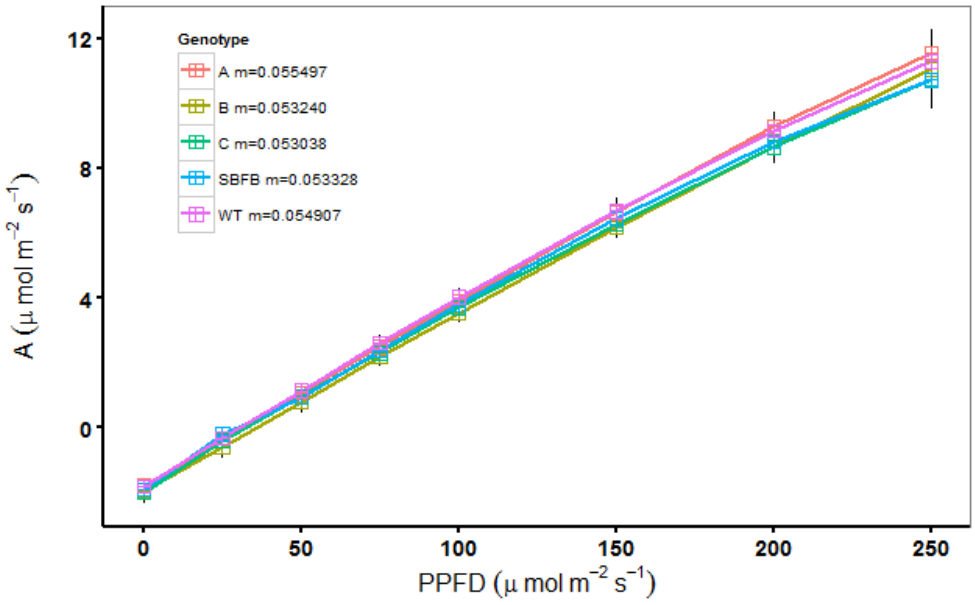

Figure 3.15. Averaged photosynthetic light response curves for the second experiment. Bars represent ± 1 s.e. of each mean (n=2). m=the slope of each curve through 200 PPFD and is representative of the maximum quantum yield ($\Phi_{CO2,max}$).

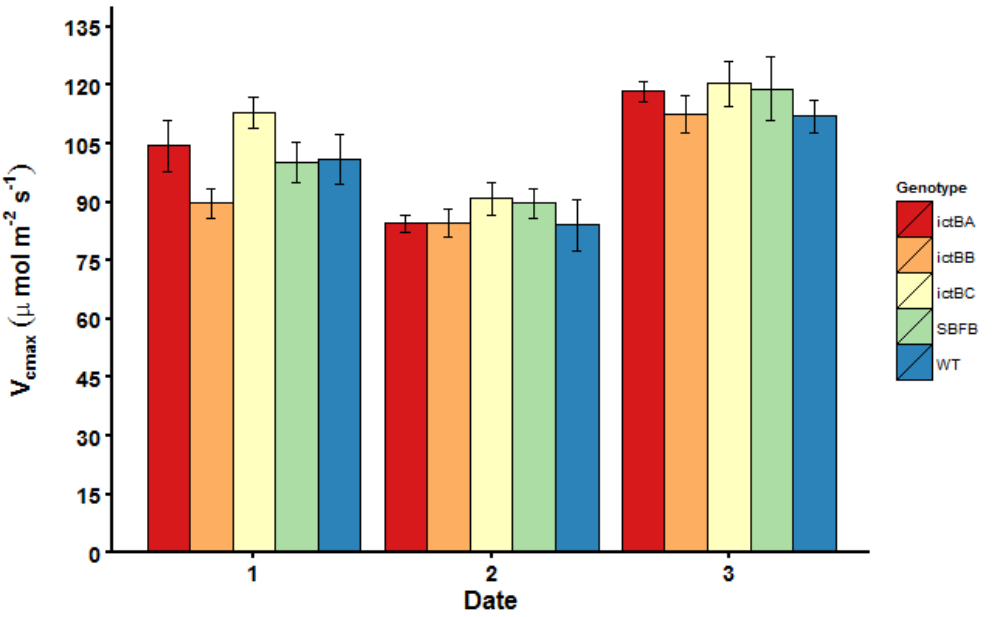

Figure 3.16. Average maximum rate of carboxylation ($V_{c,max}$) expressed in µmol $m^{-2}s^{-1}$. Date 1, 2, and 3 refer to DOY182-183, 204-205, and 226-227, respectively, in the 2014 field experiment. Bars represent ± 1 s.e. of each mean (n=3-5).

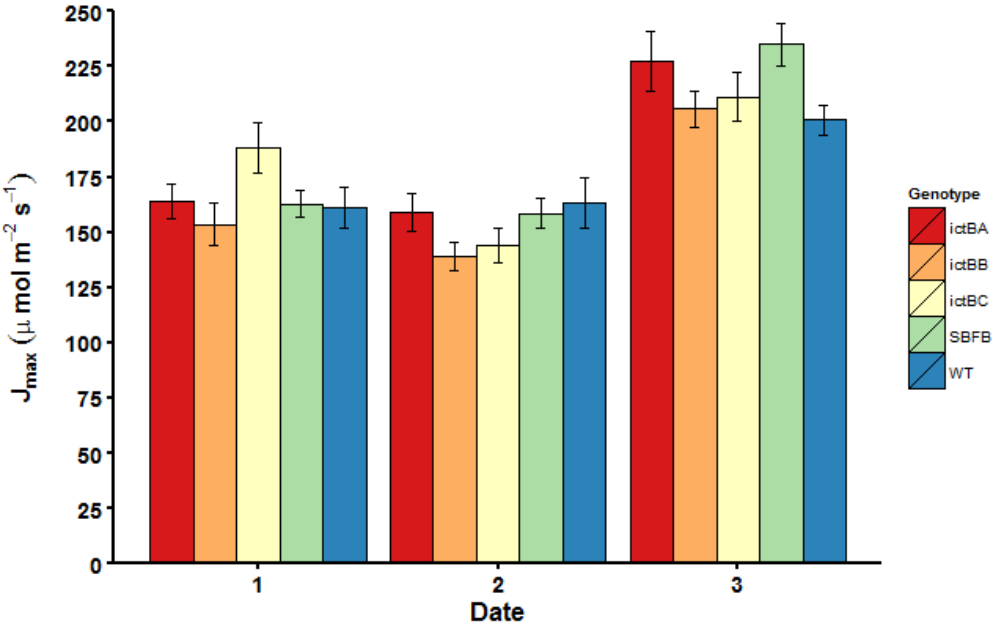

Figure 3.17. Average maximum rate of electron transport (J_{max}) expressed in µmol$m^{-2}s^{-1}$. Date 1, 2, and 3 refer to DOY182-183, 204-205, and 226-227, respectively, in the 2014 field experiment. Bars represent ± 1 s.e. of each mean (n=3-5).

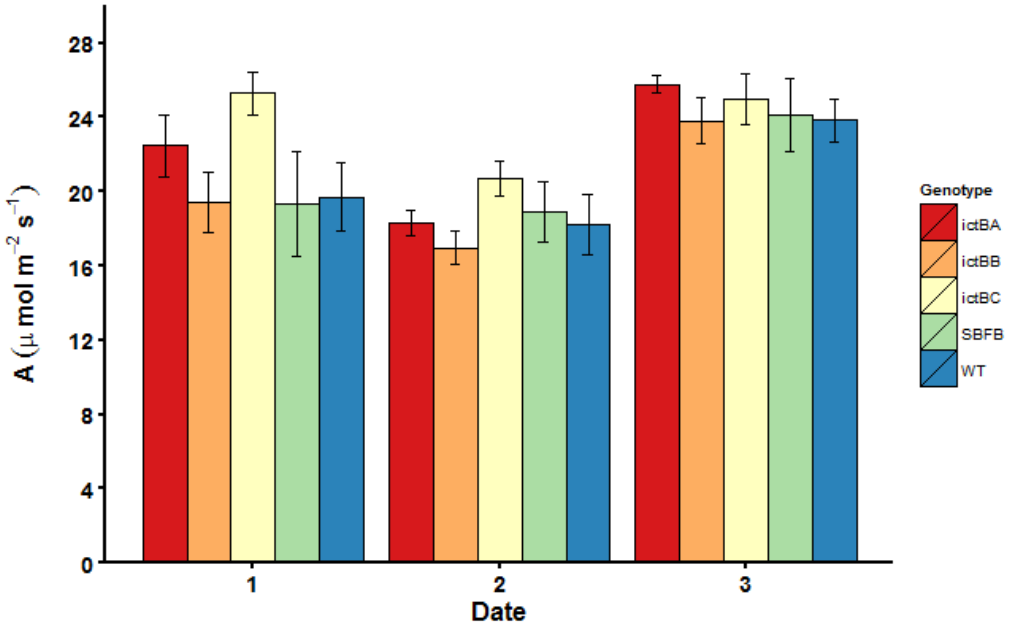

Figure 3.18. Average net photosynthetic uptake (*A*) expressed in μmolm^{-2}s^{-1} Date 1, 2, and 3 refer to DOY182-183, 204-205, and 226-227, respectively, in the 2014 field experiment. Bars represent ± 1 s.e. of each mean (n=3-5).

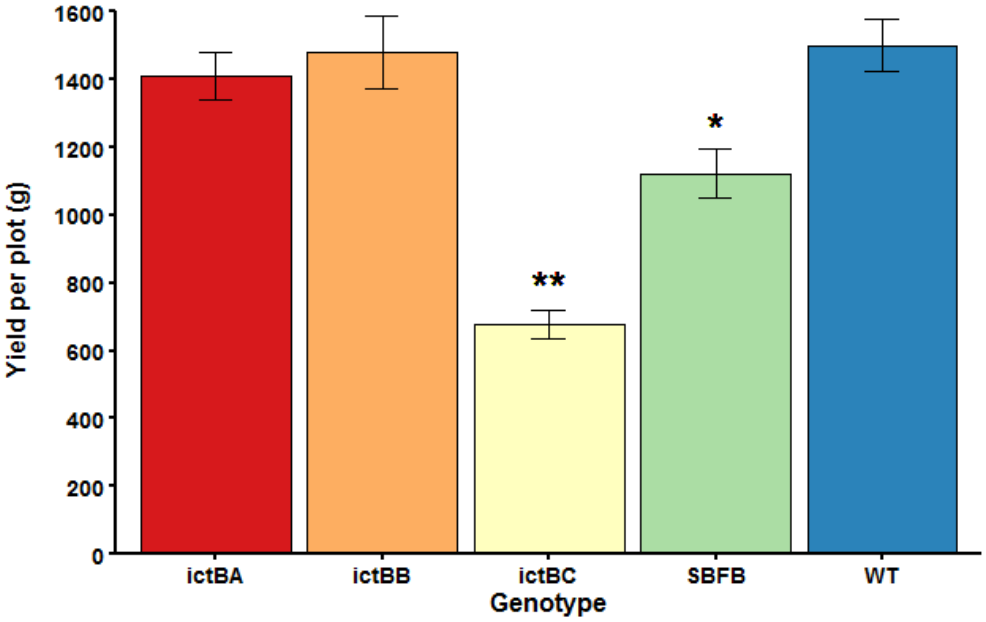

Figure 3.19. Average yield for the 2014 field experiment (* =p<0.005, ** p=<.0005). Bars represent ± 1 s.e. of each mean (n=4).

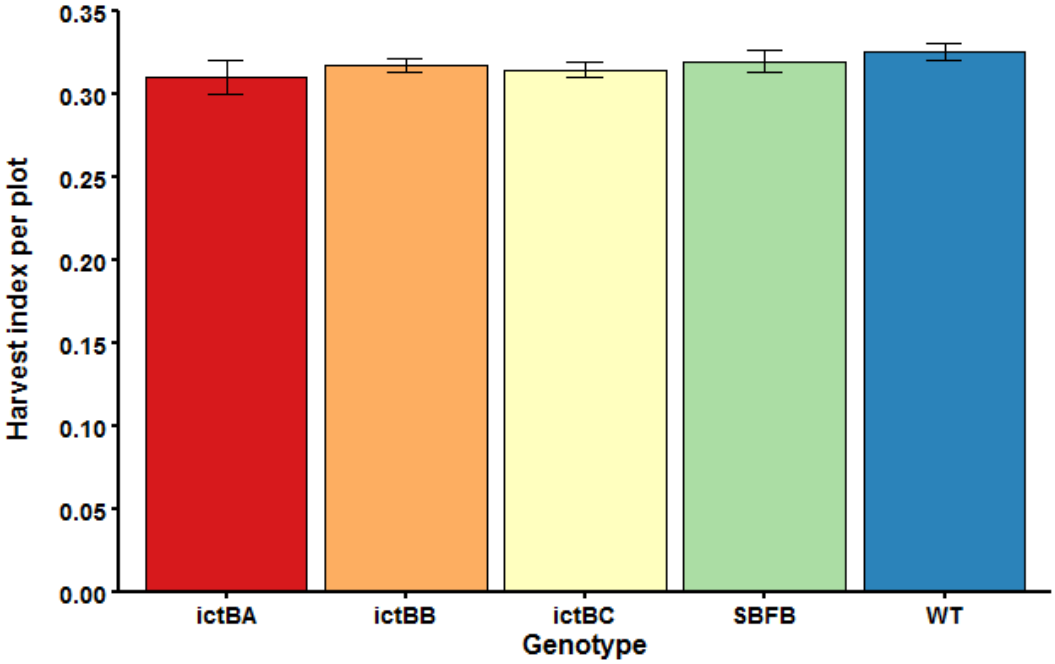

Figure 3.20. Average harvest index for the 2014 field experiment. Bars represent ± 1 s.e. of each mean (n=4).

Figure 3.21. Picture showing leaf symptoms of soybean SDS from the May 2014 field experiment.

Discussion

There were no significant differences found for any of the parameters measured in either of the controlled environment experiments. To test whether the results obtained from the controlled environment experiments were due to artificial growing conditions, a field trial was done. The 2014 growing season received more rainfall, with 25 days over the growing season (June-August) receiving more than 0.1", compared the amount of rainfall seen in the region compared to 2013, which had only 10 days receiving more than 0.1" of rain (ISWS, 2015). The 2014 growing season also showed a larger disparity between average maximum temperatures and average minimum temperatures compared to the 2013 growing season (ISWS, 2015). Due to the wet and cool conditions, Sudden Death Syndrome (SDS) was observed in most experimental plots by the R3 growth stage (Fig. 20). SDS is caused by a soil-borne fungus, *Fusarium virguliforme*, which colonizes the soybean root system early in the season but symptoms do not occur until midsummer, when promoted by wet conditions (Pioneer, 2015). Symptoms of SDS include mottling and chlorosis of the leaves and leaflet die-off and separation from the plant, resulting in smaller plants and lower yields. Due to the confounding nature of the SDS symptoms with the genetic manipulation of the soybeans, it is difficult to say whether genetic manipulation would have affected yield, however the results suggest either the transgenics were more susceptible to SDS or simply less productive, regardless of SDS. The *SBFB* and C genotypes were observed to have significantly lower yield compared to wild type, however, they maintained a similar harvest index to wild type and were also observed to have the clearest signs of SDS infection, suggesting that increased vulnerability caused the lower yield. In both the controlled environment experiments and field trial, photosynthetic parameters showed no significant differences compared to wild type, suggesting that the genetic modifications did not

affect photosynthesis and growth as predicted at ambient [CO_2]. The results for the *ictB* transformation event A discussed here are contrary to the increases in RuBP-saturated photosynthesis, final plant mass, seed yield, and leaf carbon uptake found by Hay (2012) in the T3 generation. However, the results are consistent with those found in the T4 generation (Bishop, unpublished), thus it's possible that any effects seen from *ictB* and *SBFB* have been silenced. Gene silencing is defined as a molecular process involved in the down regulation of specific genes and is thought to have evolved as a genetic defense system against viruses (Fagard and Vaucheret, 2000). Generally, this mechanism is induced by RNA silencing, in which double-stranded RNA is induced into small interfering RNAs of 21 to 25 nucleotides that correspond to both sense and antisense strands of the gene being targeted for silencing (Hamilton and Baulcombe, 1999). The small interfering RNAs then become part of a protein complex, where they will then select the target RNAs which leads to degradation (Zamore et al., 2000). RNA silencing has been used as a tool to explore the effects of downregulating key genes in higher plants for many years now, though it can also be an unintended consequence (Stam et al., 1997; Baulcombe, 2004). It appears that the transgene of the *ictB* could have been silenced after the third generation in event A. It's possible that the transgene became silenced in a later generation due to position or locus structure effects. The position of the transgene in certain repetitive DNA sequences or repressive heterochromatin could lead to silencing. Copy number, intactness, and arrangement within the gene locus can also affect stability and expression (Kohli, et al., 2010).

References

Amoroso, G., Seimetz, N., & Sultemeyer, D. (2003). The dc13 gene upstream of ictB is involved in rapid induction of the high affinity Na^+ dependent HCO_3^- transporter in cyanobacteria. *Photosynthesis Research, 77*(2-3), 127-138. doi: 10.1023/a:1025873718682

Badger, M. R., & Price, G. D. (2003). CO_2 concentrating mechanisms in cyanobacteria: molecular components, their diversity and evolution. *Journal of Experimental Botany, 54*(383), 609-622. doi: 10.1093/jxb/erg076

Baulcombe, D. (2004). RNA silencing in plants. *Nature, 431*(7006), 356-363. doi: 10.1038/nature02874

Bernacchi, C. J., Pimentel, C., & Long, S. P. (2003). In vivo temperature response functions of parameters required to model RuBP-limited photosynthesis. *Plant Cell and Environment, 26*(9), 1419-1430. doi: 10.1046/j.0016-8025.2003.01050.x

Bishop, K. (unpublished).

Bonfil, D. J., Ronen-Tarazi, M., Sultemeyer, D., Lieman-Hurwitz, J., Schatz, D., & Kaplan, A. (1998). A putative HCO_3^- transporter in the cyanobacterium *Synechococcus sp. strain PCC 7942*. *Febs Letters, 430*(3), 236-240. doi: 10.1016/s0014-5793(98)00662-0

Fagard, M., & Vaucheret, H. (2000). Systemic silencing signals. *Plant Molecular Biology, 43*(2-3), 285-293. doi: 10.1023/a:1006404016494

Hay, W. (2012). Engineering cyanobacterial genes into *Glycine max* (soybean) leads to increased photosynthesis and productivity. UIUC Ideals. Accessed 1 May 2015.

Illinois State Water Survey (ISWS). (2015). Climate Observations for Champaign-Urbana, IL. http://www.sws.uiuc.edu/atmos/statecli/cuweather/. Accessed 20 June 2015.

Jones, L., Hamilton, A. J., Voinnet, O., Thomas, C. L., Maule, A. J., & Baulcombe, D. C. (1999). RNA-DNA interactions and DNA methylation in post-transcriptional gene silencing. *Plant Cell, 11*(12), 2291-2301. doi: 10.1105/tpc.11.12.2291

Kohli, A., Miro, B., & Twyman R.M. (2010). Transgenic crop plants, chapter 7. Springer-Verlag Berlin Heidelberg. 201-237. DOI 10.1007/978-3-642-04809-8_7

Lefebvre, S., Lawson, T., Zakhleniuk, O. V., Lloyd, J. C., & Raines, C. A. (2005). Increased sedoheptulose-1,7-bisphosphatase activity in transgenic tobacco plants stimulates photosynthesis and growth from an early stage in development. *Plant Physiology, 138*(1), 451-460. doi: 10.1104/pp.104.055046

Pioneer. (2015). Soybean Insect and Disease Guide: Sudden Death Syndrome. https://www.pioneer.com/home/site/us/agronomy/crop-management/soybean-insect-disease/sds/. Accessed 27 April 2015.

Price, G. D., Badger, M. R., & von Caemmerer, S. (2011). The prospect of using cyanobacterial bicarbonate transporters to improve leaf photosynthesis in C_3 crop plants. *Plant Physiology, 155*(1), 20-26. doi: 10.1104/pp.110.164681

Sharkey, T. D. (1985). Photosynthesis in intact leaves of C_3 plants: physics, physiology and rate limitations. *Botanical Review, 51*(1), 53-105. doi: 10.1007/bf02861058

Shibata, M., Katoh, H., Sonoda, M., Ohkawa, H., Shimoyama, M., Fukuzawa, H., . . . Ogawa, T. (2002). Genes essential to sodium-dependent bicarbonate transport in cyanobacteria - Function and phylogenetic analysis. *Journal of Biological Chemistry, 277*(21), 18658-18664. doi: 10.1074/jbc.M112468200

Stam, M., Mol, J. N. M., & Kooter, J. M. (1997). The silence of genes in transgenic plants. *Annals of Botany, 79*(1), 3-12. doi: 10.1006/anbo.1996.0295

Zamore, P. D., Tuschl, T., Sharp, P. A., & Bartel, D. P. (2000). RNAi: Double-stranded RNA directs the ATP-dependent cleavage of mRNA at 21 to 23 nucleotide intervals. *Cell, 101*(1), 25-33. doi: 10.1016/s0092-8674(00)80620-0

Zhu, X.-G., de Sturler, E., & Long, S. P. (2007). Optimizing the distribution of resources between enzymes of carbon metabolism can dramatically increase photosynthetic rate: A numerical simulation using an evolutionary algorithm. *Plant Physiology, 145*(2), 513-526. doi: 10.1104/pp.107.103713

CHAPTER 4: CONCLUDING REMARKS

Kubien and Sage (2008) transformed tobacco that expressed native rubisco at 30% of wild type and found that levels of photosynthesis were consistently lower in the transformed line. This finding is reasonable because levels of rubisco activase, the enzyme required to enable rubisco to initiate the first step of the photosynthetic pathway, remain the same, while the amount of rubisco available to be activated is considerably less. Thus, it would be interesting to see if the 15% overexpression line, NL25, had the same activation rates of rubisco compared to wild type. It is known that the binding specificity for rubisco changes with temperature. Kubien and Sage also looked at how their transformed lines influenced rubisco kinetics at various temperatures and found that their results supported the prediction that high temperatures reduce photosynthesis due to a RuBP regeneration limitation, rather than the ability of rubisco activase to maintain a high level of rubisco activation. Knowing the rubisco activation rates of the lines that have an altered binding specificity for CO_2 at a range of temperatures would inform how these changes are altering rubisco kinetics on a molecular scale. This additional data would allow for better predictions of what the effects of the alteration would have on rubisco limited photosynthesis and RuBP regeneration limitation. The BicA line, which contained a bicarbonate transporter from *Synechococcus* PCC7002, was thoroughly described by Pengelly et al. (2014) in which they found no effect on chloroplast ultrastructure, photosynthetic rate, isotope discrimination, or growth.

To confirm gene expression of *ictB* in the soybean studies described here, mRNA was confirmed to be expressed, expression levels using qRT-PCR was not done. However, although there may be high levels of mRNA, it's not possible to determine whether the *ictB* mRNA is being encoded into protein because currently there is no antibody for use in a Western blot to

determine protein content. If this gene construct were to be created again, it's recommended that it be tagged with a sequence of a known antibody so that at least the tagged portion could be confirmed through qRT-PCR and Western blot. In this way, gene silencing could also be more effectively studied. The overexpression of the SBPase from *Arabidopsis thaliana* engineered into *Nicotiana tabacum* plants has been shown to stimulate photosynthesis and growth (Lefebvre et al., 2005). To test whether the bifunctional enzyme influences the regenerative capacity of the C3 cycle in a similar way to the two enzymes separately, more thorough and comprehensive studies need to be done. I would recommend silencing the native FBPase and SBPase of a higher plant, while introducing the cyanobacterial *SBFB.* This would be a difficult gene construct to introduce; however, transient assays could potentially be used to expedite the process of seeing the effects on photosynthesis. I would also recommend creating all combinations of this construct, such as silencing FBPase, introducing *SBFB*, and leaving the native SBPase to see if there are interaction effects. If plants could grow without the native enzymes, it would support the prediction that the plant could utilize the cyanobacterial enzyme in the same way it uses the two enzymes separately. Because there were no significant differences found between the one event of the *SBFB* transformation in any of the three studies that incorporated it, it's possible that the predicted benefits of the bifunctional enzyme doesn't have the same properties as the two separate enzymes found in higher plants. It's also possible that studying one event from a transformation isn't sufficient to characterize this gene's effects. In both the case of *ictB* and *SBFB*, it would be beneficial to more fully elucidate their functions in cyanobacteria before assuming the effects they would have in higher plants. Fully understanding their function and mechanism would allow for the optimization of introducing such cyanobacterial genes into higher plants. Though the genetic alterations made to the plants in this study did not have the

predicted outcomes based on previous research, this study has potentially contributed to the knowledge of which genes do and do not have strong impacts on photosynthetic capacity and efficiency.

References

Kubien, D. S., & Sage, R. F. (2008). The temperature response of photosynthesis in tobacco with reduced amounts of Rubisco. *Plant Cell and Environment, 31*(4), 407-418. doi: 10.1111/j.1365-3040.2008.01778.x

Lefebvre, S., Lawson, T., Zakhleniuk, O. V., Lloyd, J. C., & Raines, C. A. (2005). Increased sedoheptulose-1,7-bisphosphatase activity in transgenic tobacco plants stimulates photosynthesis and growth from an early stage in development. *Plant Physiology, 138*(1), 451-460. doi: 10.1104/pp.104.055046

Pengelly, J. J. L., Förster, B., von Caemmerer, S., Badger, M. R., Price, G. D., & Whitney, S. M. (2014). Transplastomic integration of a cyanobacterial bicarbonate transporter into tobacco chloroplasts. *Journal of Experimental Botany, 65*(12), 3071-3080. doi: 10.1093/jxb/eru156